



INGV
terremoti
vulcani
ambiente

ISTITUTO NAZIONALE
DI GEOFISICA E VULCANOLOGIA

Subj: Revision of the manuscript nness-2020-70: "Style-of-faulting of expected earthquakes in Italy as an input for seismic hazard modeling" written by Pondrelli S. et al.

Dear Editor,

here we submit the detailed response to the Reviewers, with explained the consequently changed we applied to our manuscript.

Main changes, out of the entire modification of the manuscript and variation requested locally by the reviewers, are:

- We added a new figure, Figure 5, that illustrates the decision-making process
- We added a cross section of focal mechanisms to better explain the tectonic style distribution at depth (included in Figure 3)
- We changed symbols in the map of results (Figure 6) to better visualize them
- We added values of the seismogenic thickness of ZS16 zones (Table S1)

You will also find a copy of the comparison of previous and present version of the manuscript. We decided for this form for the requested marked-up version, because we changed so much of our work, thanks to comments made by reviewers, that it would have been nearly completely in bold.

Best regards,

Silvia Pondrelli
Silvia Pondrelli

Bologna, July 31, 2020

Sezione di BOLOGNA

Via Donato Creti, 12

40128 BOLOGNA | Italia

Tel.: +39 0514151411

Fax: +39 0514151498

aoo.bologna@pec.ingv.it

www.bo.ingv.it

Answer to revision made by Rev1 to the manuscript “Tectonic styles of expected earthquakes in Italy as an input for seismic hazard modeling” by Silvia Pondrelli et al.

Dear Referee #1,
thank you for your useful suggestions and comments. Following the scheme you proposed us, we modified substantially the manuscript, that now has a more coherent shape.

In the following we answer point by point to your comments.

Anonymous Referee #1
Received and published: 8 May 2020

The paper presents a quite simple, but practical and original approach for assigning a generic style-of-faulting and likely nodal planes in seismogenic zones defined for PSHA. These are important parameters, particularly for the proper selection of the ground motion prediction equations to be used in the calculations as well as for the calculation of the distance to the source.

I believe this research merits to be published in NHESS but it really needs a thoroughly revision as in its present state it seems more like a draft rather than a carefully submitted manuscript.

First of all, the paper needs to be better structured, better organized. For example, line 171 and the following (the main purpose of the study) should go at the beginning (Introduction), not in the middle of the methodology section. Same with lines 131-139.

There are more examples of disorganization highlighted in the pdf attached. I strongly suggest the authors to follow a classical scientific paper structure, like: Introduction, Seismotectonic framework, Data and Methods, Results, Discussion and Conclusion. Second, I encourage the authors to make an effort using better English and, particularly, a more formal style. In the pdf attached I have highlighted across the manuscript many phrases that need to be rewritten.

We agree with the reviewer and we reorganised completely the paper following all given suggestions. Now the manuscript has the “classical” scientific paper structure.

Additionally, your writing has to be more precise and specific. Give explanations when necessary (eg, lines 133, 150, . . . and so many others highlighted in the pdf attached). We have followed this suggestion, implementing the description of all parts of the manuscript.

The following comments are organized in sections; those that a future revised version of the manuscript should contained in order to be accepted for publication in NHESS:

-Introduction section: Start stating the importance of the issue, why and how this is used in PSHA. If there are any other previous work, it should be mentioned here (and there is one, at least). Identify the problems tackled in previous work. Coherently state your objective. Highlight the originality of your approach.

An entire paragraph in the Introduction is now dedicated to the relevance that the knowledge of the style-of-faulting has in the PSHA.

We also moved and implemented here the description of previous work and motivations to go further with respect to it.

Explain what a “cascade” criteria is, what makes it better from “normal” criteria?

We removed the term “cascade”, as we used “normal” criteria for selecting the focal mechanisms.

Across the paper you are using the term “tectonic style”, which is very geological. I rather suggest you to use “style-of-faulting” which is more commonly used in PSHA literature.

We changed the term in the title and all over the manuscript following the reviewer suggestion.

-Seismotectonic framework (missing section): Additionally from what you say in your introduction, I strongly suggest to add a map of active faults of Italy (a new Figure), from the European database for example (SHARE project). Discuss the kinematics of the active faults from geological field data in each of the seismic zones with the focal mechanisms available, are they consistent?

In figure 1 we added the composite seismogenic sources taken from the Italian database DISS 3.2.1 (<http://diss.rm.ingv.it/diss/>). We also discussed the consistency between available focal solutions and seismogenic features of the seismotectonic model.

- Data and Methods (missing section): This new section could begin with your “collecting seismic moment tensors” (Data) and followed by your “Seismic Moment Tensor summation and selection criteria” (Methods).

Table 1 presents the final results, but Table 2 represents a previous process that is used to get to the results of Table 1. . . I believe that Table 2 should go before Table 1.

Yes, we agree with the reviewer. We modified the order of the Tables to have a more coherent content and a better relation with the computation and decision-making process.

I would rather use the term “reverse fault” than “thrust”. A “thrust” is a particular type of reverse fault (a low-dipping reverse fault), while “reverse” is more general for the purpose of your research and for its application in PSHA.

Done.

- Results section: This new section would include your “Tectonic Styles and expected focal solutions in the ZS16 Seismogenic Model”. The Table with the results (your Table 1) should come here.

We agree with this comment and so we modified according to the reviewer suggestion.

- Discussion section: Please, produce a proper Discussion section, independent from a Conclusion section. Start the discussion from line 282 onwards. You could add in your discussion the agreement or not between geological field data (kinematics of active faults) and your results.

Done.

- Conclusion section: You could put here lines 277-281, though more developed (for instance, you could also mention the style-of-faulting depth-dependency found, and so..). Briefly explain the style-of-faulting assigned to each major geological region of Italy.

Done.

FIGURES: The digital terrain models on the background of the figures could be much more detailed. Try to produce more attractive figures. It is compulsory to add a geographical frame (coordinates!).

Now all figures have been changed, using a better topography and a proper geographical frame.

Figure 4 has three sections, a, b and c. The foot caption should refer independently to each section. A better explanation of the graphs is needed.

We changed the caption and we improved the text with an extended explanation of the computation and meaning of dispersion, where we refer this figure.

Figure 6 needs to differentiate the three different captions with letters (a, b, c).

Done.

TABLES improve formatting (table 3 is different).

Done.

There is a typo in "Idria".

Idria is the correct name of zone n.1.

Table 1 should be 2, and conversely.

Done.

Please, double check you are using the right format when citing web pages (check the journal guidelines), and in tables and figures.

We applied all over the text the format requested by the Journal.

Check the pdf attached for more corrections and comments (highlighted in yellow).

We reviewed the manuscript following all the suggested corrections and the comments we found in the pdf.

Answer to revision made by Rev1 to the manuscript “Tectonic styles of expected earthquakes in Italy as an input for seismic hazard modeling” by Silvia Pondrelli et al.

Dear Referee #2,

thank you for your useful suggestions and comments, at which in the following we answer point by point.

Anonymous Referee #2

Received and published: 19 May 2020

The aim of this paper is to propose a procedure to characterize the predominant kinematic styles (strike, dip and rake) of each of the 50 Seismogenic Areas of the Italian Model ZS16. The authors first present the database used, which is composed of seismic moment tensors ($M_w > 4.5$) and focal mechanisms. For some events, the kinematic interpretation and the magnitude estimates rely on an existing database of seismogenic sources that is based on the interpretation of different geological and geophysical information. In the second part they present a procedure, which consists in identifying, for each seismic zone, the percentage of events in the database that fall in each kinematic style, identifying predominant nodal plane(s) based on a procedure that weighs the final focal mechanisms based on cumulated seismic moment criteria. Where necessary, total or partial random source contributions are attributed instead of specific kinematic styles.

Review

This paper represents an important preliminary step in the building of seismic hazard models that use modern GMPEs, whereby expected motions may differ considerably depending on the kinematic style of the causative fault. It deserves to be published but only after major revisions. The structure of the paper needs to be improved and the seismogenic depth parameter of the reference Italian Model ZS16 better discussed;

We changed several parts of the manuscript following the reviewer suggestions, adding in the Introduction why it is important to define the style-of-faulting as a support to variations in the expected ground motion.

We also added a new section entitled “Seismotectonic framework”, with a paragraph describing ZS16 and how the seismogenic depth adopted have been determined.

introductory paragraphs should be re-grouped in the introduction;

Done.

explanations for how the database was constructed better justified (e.g. why the CPT115 magnitude is not used?);

We better explained the process of construction of our dataset. The main scope of this work was to evaluate average focal mechanisms for each zone, and to reach this aim we created a dataset of available focal mechanisms. The magnitude, depth and nodal planes of a focal mechanism are correlated, therefore, when possible, we maintained all these information from original databases, instead of using estimates of the magnitude derived from combinations of different agencies (e.g., ISC, INGV bulletin, CMT). In addition, it is worth to note that a unique database including all the used earthquakes (and focal mechanisms) does not exist, whereas CPT115 magnitudes also derive from the CMT Italian Dataset for all the common events.

final selection of events actually used for the computation of the predominant kinematic styles (strike, dip and rake) should be easily accessible to the reader (see comments for Table1suppmat).

We agree with the reviewer suggestion and we modified the Table S2 in the Supplementary Material adding also the number of the seismic zone at which each event belongs (if any).

The weighting procedure could be better illustrated, in particular for regions where the final result may potentially be driven by just the biggest event in the zone.

Any cumulative solution is unavoidably weighted with the greatest events. On the other hand, we are looking for the dominating style-of-faulting that in general is the one of the greatest event. However, to avoid the lost of minor style-of-faulting we proceeded with the separation of the dataset in the three main families of tectonic styles before computing the cumulative ones. We evaluated the cumulative seismic moment for each tectonic style within each zone and we used these values to weight their relative contribution. A style-of-faulting is taken into account if it contributes for at least the 10% of the total cumulative seismic moment of the zone. For example, in the zone n.18 (Lunigiana-Casentino), the final results is 30% NF (normal fault) and 70% SS (strike-slip) because nearly the 30% of seismic moment released in this area is given by normal fault events (2) and nearly the 70% by strike slip events. A minor reverse fault components is not included in the final solution because given by one event only, contributing to the total seismic moment of zone n.18 for a percentage lower than 10%.

To better illustrate our decision-making process we also added a new figure, Figure 5.

Finally, I would suggest adding uncertainties in strike, dip and rake to Table 2, reflecting the color scheme in Figure 2 and providing end-users with a measure of dispersion for each zone.

The only uncertainty we can attribute to these values is the amount of dispersion of P- B- and T- axes position of single focal mechanisms before the summation with respect to the distribution of the axes of the cumulative one. We already computed it, to select when a cumulative focal mechanism can be considered robust (see Figure 4). This computation and evaluation has been implemented in the manuscript and values of dispersion are reported in the new Table 2.

Additional requests/suggestions:

1. Abstract

The abstract mentions that uncertainties in the attribution of kinematic styles would be quantified. At present this is not the case. See comments below.

The abstract, as most of the manuscript has been rewritten following this suggestion.

2. Structure of the paper

Line 150- Entire paragraph needs re-writing: I suggest you shift all “introductory” material to the introduction, present how seismogenic depths proposed in the reference ZS Model are used or not in the selection of events used in Table 1.

The paper has now a complete different structure, following all these suggestions.

3. Database – Choice of Magnitudes

Line 115 – “Considering the high magnitude of these events (1905 M6.9 in Calabria and the 1915 M6.9 in the Southern Apennines) and the aim of this study, we looked for quaternary tectonics information in the DISS database (DISS Working Group, 2018), according to which the seismogenic sources of both events are described as pure extensional, based on

geological studies (e.g. Loreto et al., 2013 for the 1905 Calabria earthquake; Galli and Galadini, 1999 for the 1915 earthquake) Could you locate these two events on a Figure and indicate a reference to the DISS ID used. I found information about these two events in the online version of CPTI15, which presents quite different magnitude estimates:

In Table1 sup material:

- o D190509080143A 1905-09-08 Mw6.8

- o D191501130652A 1915-01 Mw 6.6

In DISS:

- o ITCS110 Sant'Eufemia (1905) Mw 6.8

- o ITCS025 Salto Lake-Ovindoli-Barrea (1915) Mw 6.7 In the CPTI15 database:

- o 1905 Calabria centrale Mw 6.95

- o 1915 Marsica Mw 7.08

This is quite confusing. Mmax being a critical parameter for defining seismogenic potential you may want to clarify your procedure or, in any case, justify why you consider DISS rather than CPTI15 as a reference for Magnitude estimates of historical earthquakes.

Thanks to suggest to add the DISS ID for sources we used, it is a relevant information we forgot to include. For the 1905 earthquake is the ITIS002, Fucino Basin Individual Source, and for the 1915 is the ITIS139, Sant'Eufemia. However from DISS we exported only the strike, slip and rake from the Individual Source Parameters list, while magnitude and seismic moment still remained those from EMMA database, because determined with seismological recordings, as well as all other data we were using. All these information are now included in the manuscript.

Essentially, the magnitude for all the events we included in our dataset is the one attributed them in the Catalogue from which they have been extracted. Our collection started from the Italy dataset and RCMT catalog, so for all events coming from there we used the "RCMT" Mw. Then we added data from other datasets (i.e. EMMA, ETH, GFZ) and for all of them we used the Mw originally given. And so we have done for 1905 and 1915 events, at which we only included the strike dip and rake extracted by Individual Sources of the DISS.

The reason because we did not use the CPTI15 magnitude is explained above and, particularly for the two mentioned earthquakes, the CPTI15 magnitudes result from merging early instrumental determinations with macroseismic estimates. Your suggestions related to the CPTI15 and Mmax would be certainly valid in the frame of a study where the seismic moment release is involved, but here we use the values of magnitudes just as a threshold to select data entry.

4. Database -Choice of depths -

Given that the ZS Model is the reference, you may want to comment on the depths currently used in the ZS model to justify for the final depth range used to select events determining the kinematic styles of each zone. For example: Line 158 "in some zones the most representative seismicity is deeper, thus we used a thickness of 40 km to ensure the inclusion of all crustal seismicity" –does this depth correspond to definition of depth in the ZS model?

We have better explained this point in the manuscript. The seismogenic thickness in the ZS16 was evaluated from the depth distribution of instrumental seismicity (i.e. the range 5° - 95° percentiles of the distribution) and the process and results are now explained in the manuscript and in Table S1. However, out of zones for which we found a variation of the

tectonic style with depth, we used all the focal mechanisms within 40 km of depth, for conservative reasons, that means to avoid the lack of any selected events.

a. Deeper zones may have different geometries than superficial zones: can you justify prolonging the same geometrical boundaries of superficial zones to the deeper zones?

We do not have geological details to build complex 3D models of the deeper zones.

Therefore, in the case of coexistence of different style-of-faultings at different depths located on the same plane projection, we have to assume the same geometrical boundaries.

Of course, this does not mean we are using the same faults as causative of shallow and deep seismicity. For example, shallow seismicity in the Apennines is almost pure normal and it is related to faults different from the deeper strike-slip/reverse faults. In this particular case, the shallow expression of the deepest faults is located in the eastern side of the Apennines. To better explain the kind of structure and tectonic style distribution in this region, we added in Figure 3 a section of focal mechanisms.

b. Shouldn't there be a deeper zone to represent the Calabrian subducting plate? The ITSD001 in the DISS database, corresponding to the "the Calabrian subducting slab", suggests a seismogenic zone between 10 and 50 km with pure thrusting kinematics. Your procedure leads to a strike-slip/normal kinematics between 0 and 40 km depth (e.g. ZS 41, ZS 39). This difference of definition in terms of seismogenic "volume" and kinematic styles between DISS and your proposal may be worth discussing.

The kinematics resulting from our study derives from the analysis of available focal mechanisms between 0 and 40 km of depth, while the ITSD001 kinematics was inferred from tectonic and structural information.

I interpret ITSD001 of DISS as a deforming zone and not a seismogenic zone. It includes all Individual Seismogenic Sources (ISS) located in Calabria and in the Ionian Sea. In Calabria all ISS are normal or (minor) strike-slip faults. In the Ionian Sea the ISS are considered mainly reverse structures. Our zone n.39 include mainly the Tyrrhenian side of Calabria and most of Calabrian territory inland, where, looking to DISS too, normal faults prevail. Thus we do not consider surprising that also earthquakes behave in the same way. It is different the result for zones n. 40 and 41 where in fact strike-slip faulting prevails from earthquakes.

Another information to underline is that we take into account only crustal seismicity that affects PHSA, we are not interested in deep seismicity.

5. Procedure - Uncertainties -

I'm surprised to see a unique value (strike, dip, rake) triplet attributed to each source zone in Table 2. Are you suggesting to use just this single value in hazard computations? Shouldn't uncertainties be associated to such estimates, quantified in Table 2 and used in hazard computations?

We proposed an evaluation of the dispersion of each cumulative solution and then we used this parameter to select/weight the results. In particular, in zones with a large dispersion, we opted for an undefined fault style (what we define random component in final results). We added these values in the new Table 2, but they are not a measure of the uncertainty. We consider this parameter important to evaluate the robustness of the results given the input focal mechanisms. We added to the manuscript an implemented explanation of this point. In any case, we suppose that a range of variability around the single triplet we computed should be qualitatively assigned by the end-user, taking into account the dispersion of the input data.

Unfortunately, it is worth to note that quantifying the uncertainties in strike-dip-rake is still an open topic.

- In the discussion, could you address the sensitivity of your procedure to the presence of very high magnitude events in some source areas in the final attribution of kinematic styles (Table 2)? One information that may be useful for the discussion is to also indicate which event contributes most to the total seismic moment in the source zone (for the zone of the 1905 earthquake, for example).

We described for each zone the event that mostly contributes, if any.

In fact, any cumulative solution is just the sum of all moment tensor of all selected events (Kostrov, 1974). Any weighting is done simply by the seismic moment: the bigger it is the more it weights. Always taking into account that we were looking for the prevailing fault style, the greatest earthquake of each zone is commonly considered the most representative.

- line 125 Knowing that for some regions the possible largest earthquake may not be represented in the available observations, how would this impact the procedure you propose?

It is a declaration of one limit of the input dataset rather than a limit on the procedure.

Looking for the prevailing fault style we need information on the focal solution of past events, and we are aware that for great earthquakes of the past we cannot obtain this information. So, it impacts not on the procedure but it should be taken into account together with other uncertainties when our results are used in hazard model computations as for instance the fact that also in historical catalogs, even if the represented time window is long (e.g. in the CPT115), possible older big earthquakes may lack.

By the way, taking into account the long time that geological process last, we can consider that where we have focal mechanisms for recent events, they are “geologically” coherent even with past earthquakes. A greater uncertainty should be taken into account for regions where recent events are absent but we know that in the past great quakes occurred. In Italy we do not find similar examples, excluding perhaps Eastern Sicily where occurred the biggest 1683 event, isolated and unique for our knowledge.

All this explanation are also included in the manuscript now.

- Line 160-168 - list the 3 zones for which a separate deeper kinematic style is defined: 19d Tuscany-Emilia Apennines Deep; 20d Emilia Deep; 25d Inner part of Marche (this one is not plotted in Figure 5)

Now they are explicitly described. However the 25d result was plotted with a too small blue circle with a black border. So we changed symbol dimension in Figure 6 (previously Figure 5) to better visualise the results.

6. Figures

Figure 1: There is a clear SW-NE alignment of deeper events between latitude 41 and 42, on the eastern coast of Italy which cuts across source zone boundaries ZS34 and ZS35. Are these characterized in the Italian Model ZS16 by some deeper sources not shown in Figure 1 or are they excluded in further analysis? Please comment.

The alignment is just apparent. Looking to a map of seismicity that includes also small magnitude events you would find a different image.

As concern exclusions, we only excluded focal mechanisms for events with a hypocentral depth greater than 40 km. That means that for most zones (see Table 1) only yellow focal mechanisms mapped in Figure 1 have not been included in the summation.

Figure 2: The label says “the entire available dataset in black”..but I no longer see the same alignment as in Figure 1, are some events excluded in this Figure?

The reviewer is right. We reported only data with a hypocentral depth within 20 km because it is the example of a summation using a 20 km seismogenic layer thickness for all the seismic zones. Now we changed the caption with an appropriate description.

Figure 5: 25d Inner part of Marche is not plotted

It was plotted, but unfortunately so small that was not visible. We changed symbols now to have a better visualisation of results in Figure 6 (previous Figure 5).

7. Tables

Table 2 should contain a measure of the dispersion associated to each evaluation which should correspond to the color scheme used in Figure 2

The results reported in Table 2 are different from what is shown in Figure 2. In Figure 2 is reported an example of the result of the summation with a seismogenic thickness of 20 km only. It represents a preliminary result of our trials to set the best seismogenic thickness to be used successively. The different colours attributed to cumulative solutions of Figure 2 is related to the amount of focal mechanisms summed in each zone and their heterogeneities. Only later, after having split the dataset of each zone in the three main tectonic styles, we determined the dispersion of each cumulative solution, those reported in Table 2.

We changed also the description of this step of the work, to avoid further misunderstandings.

Table 1SuppMat - should contain the source zone ID for each event used to apply the procedure, the events excluded because too deep will have no ID. . .and should not be shown in Figure 1.

We added the number of the source zone in the S2 table so to easily identify those included or excluded. We anyway decided to let them in Figure 1 because we consider this collection particularly interesting and we prefer to show it.

8. Mistakes

Line 50: "a narrow bend striking" you mean "narrow band"?

We corrected the typo.

Line 69" geological databases, such as DISS", DISS is defined on the web site as a database of "seismogenic sources" not of fault sources nor geological sources

Yes, the definition of DISS is the Database of Individual Seismogenic Sources. Our expression is due to the fact that the seismogenic sources we extracted from DISS to implement our dataset are defined on the base of geological studies. Moreover, a large number of seismogenic sources included in DISS have the same origin, defined on the base of geomorphological studies aimed to find traces and effects of faults at the surface, or paleoseismic studies, or analysis of traces of faults cutting the surface and related to a single earthquakes. Among all catalogs used in studies like our one, DISS is considered more geological than for instance a focal mechanism catalog.

Table 1SuppMat: "The ID of each event starts with a letter that identifies"- missing the end of the table caption?

The reviewer is right. Now it is completely readable.

Line 146 "because they do not include any seismic event with magnitude greater or equal than M 4.5"-suggestion: "because no events with $M \geq 4.5$ are present"

We applied the change.

Line 150: “.. the depth distribution of the Italian seismicity (Figure 1), it becomes immediately evident” - it is not really immediately evident. You may want to rephrase
We changed all this part to give a better description of seismicity distribution.

Style-of-faulting Tectonic styles of expected earthquakes in Italy as an input for seismic hazard modeling

S. Pondrelli¹, F. Visini², A. Rovida³, V. D'Amico², B. Pace⁴ and C. Meletti², ~~ilvia Pondrelli⁴,
Francesco Visini², Andrea Rovida³, Vera D'Amico², Bruno Pace⁴ and Carlo Meletti²~~

(1) Istituto Nazionale di Geofisica e Vulcanologia, Sezione di Bologna, Italy,

(2) Istituto Nazionale di Geofisica e Vulcanologia, Sezione di Pisa, Italy,

(3) Istituto Nazionale di Geofisica e Vulcanologia, Sezione di Milano, Italy,

(4) ~~DiSPUTer Department~~~~partimento di Scienze Psicologiche, della Salute e del Territorio~~
(DiSPUTer), Università G. d'Annunzio Chieti-Pescara, Chieti, Italy

Abstract

~~The style-of-faulting and distributions of nodal planes are an essential input for probabilistic seismic hazard assessment. As a part of a recent elaboration of a new seismic hazard model for Italy, we defined criteria to parametrize the style-of-faulting of expected earthquake ruptures and evaluate their representativeness in an area-based seismicity model. Using available seismic moment tensors for relevant seismic events ($M_w \geq 4.5$), first arrival focal mechanisms for less recent earthquakes and also geological data on past activated faults, we collected a database for the last ~100 yrs, gathering a thousand of data all over the Italian peninsula and regions around it. On this dataset we adopted a procedure that consists, in each seismic zone, of separating the available seismic moment tensors in the three main tectonic styles, making summation within each group, identifying possible nodal plane(s), taking into account the different percentages of style-of-faulting and including, where necessary, total or partial (even in terms of tectonic style) random source contributions. Referring to the used area source model, for several seismic zones we obtained robust results, e.g. along the central and southern Apennines we expect future earthquakes to be mostly extensional, although in the outer part of the chain reverse and strike-slip events are possible. In the Northern part of the Apennines we expect different style-of-faulting for different hypocentral depths. In zones characterized by a low seismic moment release, the possible style-of-faulting of future earthquakes is less clear and it has been represented using different combination of random sources.~~

~~ectonic styles and distributions of nodal planes are an essential input for probabilistic seismic hazard assessment. As a part of a recent elaboration of a new seismic hazard model for Italy, we adopted a cascade criteria approach to parametrize the tectonic style of expected earthquake ruptures and their uncertainty in an area-based seismicity model.~~

~~Using available or recomputed seismic moment tensors for relevant seismic events (M_w starting from 4.5), first arrival focal mechanisms for less recent earthquakes, and also geological data on past activated faults, we collected a database for the last ~100 yrs gathering a thousand of data all over the Italian peninsula and regions around it. The adopted procedure consists, in each seismic zone, of separating the available seismic~~

moment tensors in the three main tectonic styles, making summation within each group, identifying possible nodal plane(s) taking into account the different percentages of tectonic styles and including, where necessary, total or partial random source contributions. Referring to the used area source model, for several seismic zones we obtained robust results, e.g. along the southern Apennines we expect future earthquakes to be mostly extensional, although in the outer part of the chain strike-slip events are possible. In the Northern part of the Apennines we also expect different tectonic styles for different hypocentral depths. In zones characterized by a low seismic moment release, the possible tectonic style of future earthquakes is less clear and it has been represented using different combination (total or partial) of random sources.

Introduction

The determination of the style-of-faulting in seismicity models for Probabilistic Seismic Hazard Assessment (PSHA) represents the key ingredient to define the orientation and the kinematics of the seismic source. The orientation, i.e. strike and dip, impacts the source-to-site distance whereas the kinematics, i.e. the rake, is linked to the choice of the coefficients of the Ground Motion Prediction Equations (GMPE), that take into account the style-of-faulting. The comparison of ground motions produced by reverse, strike-slip or normal faults shows that reverse-faulting events generate higher amplitude motions, especially with respect to normal faulting ones (e.g. Bommer, 2003). According to Bindi et al. (2011), in the case of the Italian strong motion data, the main differences in the ground motion result over the medium-to-short period range ($T < 1$ s), where the expected values for a reverse mechanism are significantly larger than those produced by the other styles of faulting. As concerns the source orientation, changing the strike of the fault leads to an increment/reduction of the rupture-to-site distance. For instance, in the case of a normal fault with M_w 6.3, the GMPE by Bindi et al. (2011) shows that increasing the distance from 20 to 30 km reduces the mean expected Peak Ground Acceleration (PGA) of about 40%. The seismotectonic setting of Italy shows the presence of all tectonic styles: normal, compressive, strike-slip and the combination of them (Figure 1).

In the Alps, the most seismically active part of the belt is to the east, where the south-verging Alpine thrusts mix with the strike-slip Dinaric structures.

Along the entire Apennines a shallow extensional tectonics dominates along the watershed, up to the Calabrian Arc and in N-NE Sicily. On the outer part of the chain, on the Adriatic side, a bit deeper compressive tectonic occurs in correspondence with the northern Apennine arc, becoming strike-slip to transpressive moving south, in correspondence of the outer part of the southern Apennines, i.e. in the Gargano Promontory. Off-shore of the northern coast of Sicily, in the southern Tyrrhenian Sea, a continuous compressive system is active west of the Aeolian islands, where the tectonic style becomes mainly strike-slip along a narrow bend striking about NS, up to the Etna volcano.

These well-studied and well-known seismotectonic features may be used to define important

characteristics of the seismic sources, for example the prevailing tectonic style to be considered in seismic hazard evaluations. Indeed, a different kind of seismic source, i.e. strike-slip or normal or thrust, produces a different shaking scenario. Tectonic style and nodal planes of expected seismicity are modelled as a distribution of nodal planes, i.e. one (or several) instances of the following set of parameters: strike, dip and rake. Actually, strike and dip are used to build the 3D geometry of the finite fault representing the seismic source, whereas rake is the parameter used to select the coefficients of ground motion predictive models that take the source into account (normal, reverse or strike-slip).

Although orientation and kinematics of the finite ruptures are a key ingredient for PSHA, there are no standard objective approaches for defining the style-of-faulting in tectonic regions, and this is generally reminded as an analysis of available fault mechanisms and a comparison with mapped active faults. Roselli et al. (2017) defined the style-of-faulting on a regular grid in Italy. They used a smoothed 2D approach started from the computation, for each cell, of a cumulative focal mechanism obtained with a weighted summation of previous focal mechanisms. However, in general, the lack of a seismotectonic model behind the calculation can affect the results, especially in small areas characterised by the coexistence of normal, reverse, and strike slip tectonics. In addition the variation of each style-of-faulting with depth should be detected and taken into account where possible. To reach this purpose, the first step is to collect the necessary data, that in this case are substantially the focal mechanisms of earthquakes with a relevant magnitude with respect to an active tectonic system, e.g. at least Mw 4.5 for Italy. The Italian peninsula is so deeply studied from this point of view, that several catalogs and databases of seismological and geological data are available, with data for the necessary magnitude interval, e.g. the European Mediterranean RCMT Catalog (Pondrelli and Salimbeni, 2015 and reference therein; doi: 10.13127/rcmt/euromed). Moreover, to increase as much as possible the time interval covered by the data, a large amount of information on source parameters concerning strong earthquakes in the last ~100 yrs is available also in geological databases, such as DISS, the database of seismogenic sources for events with M greater than 5.5 in Italy (DISS working group, 2018; <http://diss.rm.ingv.it/diss>).

Our objective is to define an approach based on seismotectonic zones, because it allows including possible variability in the style-of-faulting with depth and preventing undesired rotations of average focal solution in case of transitions to different kinematics at the surface or at depth. Meletti et al. (2017) released a seismogenic zone model, named ZS16, that represents the update of the ZS9 model (Meletti et al., 2008) adopted by the current reference seismic hazard model of Italy (Stucchi et al., 2011). ZS16 is based on the same seismotectonic knowledge used for designing ZS9, but includes many new data available for the study area (earthquake catalog and fault database among others) that allow a better definition of the boundary and of the seismogenic depth of each seismic source zone.

In this paper we illustrate the selection and weighting criteria to gather a representative dataset of nearly 100 years of focal mechanisms in Italy, and the procedure we tested and applied to define the style-of-faulting using the recently produced ZS16 seismotectonic zoning for the update of the national PSHA for Italy.

Seismotectonic framework and seismogenic zones

Here we describe the data selection and the obtained dataset, the different trials in cumulative moment tensors computations that helped to identify some useful and important source parameters and the procedure applied to individuate the expected faulting mechanism for each of the seismic sources in a new area source model for Italy, that hereinafter we refer to as the Seismogenic Area-based Model ZS16 (Meletti et al., 2019).

The seismotectonic setting of Italy shows the presence of all tectonic styles: normal, compressive, strike slip and the combination of them (Figure 1). In the Alps, the most seismically active part is the eastern one, where the south verging Alpine thrusts meet the strike slip Dinaric structures, and where the famous 1976 Friuli seismic sequence included several great to moderate earthquakes with reverse and strike-slip focal mechanisms (Pondrelli et al., 2001). Moving towards the south, along the entire Apennines watershed, a shallow extensional tectonics dominates, as testified also by the seismic sequences of 1997-1998 Umbria-Marche, of L'Aquila 2009 and the recent 2016-2017 Central Italy (Figure 1; Chiarabba et al., 2018 and references therein). This normal tectonic style continues up to the Calabrian Arc and in N-NE Sicily. However, on the outer part of the chain, on the Adriatic side, compressive tectonic occurs in correspondence with the northern Apennine arc, and the 2012 Emilia seismic sequence was its most recent expression (Anzidei et al., 2012). To the south, tectonics becomes strike slip to transpressive in correspondence of the outer part of the southern Apennines, i.e. in the Gargano Promontory (Figure 1). Another characteristic of the seismicity of the Adriatic side of the peninsula is a general greater hypocentral depth of the earthquakes, so to have not only a lateral variation of the dominating tectonic style, but also with depth. Crossing the Messina strait, that separates Calabria from Sicily, we still find a shallow extensional seismicity along the mountains watershed, that is however a less persistent feature. In fact in Sicily other tectonic styles prevail, as for instance the north-south narrow bend from Aeolian islands up to the south of Mt. Etna, which is densely populated by strike-slip earthquakes, or the active compressive front west of the Aeolian islands, offshore northern Sicily in the southern Tyrrhenian Sea (Figure 1). This quick overview of the seismotectonic characteristics of the Italian peninsula is based on seismological and geological data, strictly related to what happens at crustal depth and thickness; in fact the subduction system and related deep seismicity active beneath the Calabrian arc and the southern Tyrrhenian sea is here excluded because we focus on shallow seismicity responsible for seismic hazard.

Collecting Seismic Moment Tensors

Meletti et al. (2019) defined a seismotectonic zoning, named ZS16, reflecting the structural tectonic framework of Italy, that we adopt for our study. It is composed of 50 area sources representing regions of spatially uniform occurrence of seismicity (Figure 1 and Table S1). To define the borders of the zones, and the upper and lower bounds of the characteristic seismogenic depth, data from mapped active faults (DISS Working Group, 2018), that played a major role, have been integrated with earthquake catalogues (Rovida et al., 2016), geodetic strain data (Devoti et al., 2016) and focal mechanisms (Global CMT, Ekström et al., 2002; European Mediterranean RCMT Catalog, 2020). In order to estimate the upper and lower seismogenic depths of the ZS16 zones for the earthquakes above the threshold relevant for the PSHA, the instrumental catalogue prepared for the recent elaboration of a new seismic hazard model for Italy (MPS19 Project) has been used (Gasperini et al., 2016).

Earthquakes with fixed depth have been removed from the reference dataset; only earthquakes that likely occurred within shallow crust, with a maximum depth of 40 km, have been included. The 5th and 95th percentile of the cumulative depth distribution of the selected dataset have been assumed as the upper and lower boundaries of the seismogenic layer depth. Finally, the definition of the upper and lower depths is reached comparing the percentiles resulting from catalogues with different minimum magnitudes (from Mw 2 to Mw 4) with the depth of the composite seismogenic sources from DISS 3.2.1. In Table S1 the obtained depth values used in ZS16 for the 50 area sources are listed.

To collect the representative dataset useful to define the different seismotectonic styles for the Italian peninsula, we started from the best quality moment tensors available, that is the CMT Italian Dataset (<http://rcmt2.bo.ingv.it/Italydataset.html>; Pondrelli et al., 2006; doi:10.13127/rcmt/italy). It is a continuously updated merge of the existing Global CMTs (Dziewonski et al., 1981; Ekström et al., 2012) and European-Mediterranean RCMTs data (Pondrelli et al., 2002; Pondrelli and Salimbeni, 2015; doi:10.13127/rcmt/euromed), including all moment tensors available for earthquakes with $M \geq 4.5$ in the time interval from 1976 to 2015.

To reach the best homogeneity in terms of spatial distribution, we added the moment tensors of a few $M \geq 4.0$ earthquakes occurred in the Alpine region where nothing else was available, obtained by seismic data inversions and belonging to the GFZ and ETHZ datasets (Bernardi et al., 2004; Saul et al., 2011).

To get a longer dataset in terms of time, we considered also first polarities focal solutions selected from the EMMA Database (Database of Earthquake Mechanisms of the Mediterranean Area, Vannucci and Gasperini, 2004). Such data have been used when they were the only available ones, thus mainly for relevant events occurred before the digital era of seismological data, as for instance the 1968 Belice (Sicily) earthquakes. In a few cases, for a single event, multiple focal mechanisms were available. To choose among them we applied the quality evaluation given in the EMMA Database, e.g. we choose the so-called “preferred” solutions. Moreover, we also took into account the following features: 1) first arrival focal mechanisms are often different from seismic moment tensor focal mechanisms (see the astonishing example of the $M 6.0$ Amatrice earthquake, Central Italy, August 24 2016 in Figure 2 of Marchetti et al., 2016); 2) first arrival focal mechanisms represent the initial fault slip, while seismic moment tensors describe the entire seismic source; the complete seismic source may be considered the most representative indicator of the tectonic style dominating the epicentral region.

For two great events of the past century, the 1905 $M 6.9$ in Calabria and the 1915 $M 6.9$ in the Southern Apennines, several first arrival focal mechanisms available in the EMMA Database are however of low quality, different among them and indicate a tectonic style different from that expected for their epicentral regions. In the EMMA Database, for both these

earthquakes, none of the “preferred” solutions, nearly strike-slip, was considered reliable enough for this study. The strike-slip kinematic seems far to be compatible with the crustal tectonic style of the Southern Apennines and Calabria regions, usually described as extensional (e.g. D’Agostino et al., 2011). Considering the high magnitude of these events and the aim of this study, we looked for quaternary tectonics information in the DISS database (DISS Working Group, 2018), according to which the seismogenic sources of both events are described as pure extensional, based on geological studies (e.g. Loreto et al., 2013 for the 1905 Calabria earthquake; Galli and Galadini, 1999 for the 1915 earthquake). Thus, lacking a stable instrumentally measured seismic focal mechanism solutions, for these two earthquakes we used seismic moment tensors reconstructed from geological data stored in the DISS database, attributing to both events an extensional seismic source.

The final dataset (Figure 1 and Table S1 in the Supplementary Material) includes nearly 1000 focal mechanisms for crustal earthquakes (with maximum 40 km of hypocentral depth), representative of about 100 years of seismicity of the Italian peninsula.

We are aware that for some regions the possible largest earthquake could be not represented in the available observations.

Data and Methods

Here we describe the building of the focal mechanism database and the procedure applied to evaluate the prevailing style-of-faulting.

Seismic Moment Tensor summation and selection criteria

Data

To collect the representative dataset useful to define the different seismotectonic styles for the Italian peninsula, we started from the best quality moment tensors available, that is the CMT Italian Dataset (CMT Italian Dataset, 2020; Pondrelli et al., 2006). It is a continuously updated merge of the existing Global CMTs (Dziewonski et al., 1981; Ekström et al., 2012) and European-Mediterranean RCMT data (European Mediterranean RCMT Catalog, 2020; Pondrelli et al., 2002; Pondrelli and Salimbeni, 2015, including all moment tensors available for earthquakes with $M \geq 4.5$ in the time interval from 1976 to 2015 included in the geographical window with latitude from 35° to 48°N and longitude from 6° to 20°E . To reach the best homogeneity in terms of spatial distribution, we added the moment tensors of a few $M \geq 4.0$ earthquakes occurred in the Alpine region, obtained by seismic data inversions and belonging to the GFZ and ETHZ datasets (Saul et al., 2011 and Bernardi et al., 2004 respectively).

To get a longer dataset in terms of time, we considered also first polarities focal solutions selected from the EMMA Database (Database of Earthquake Mechanisms of the Mediterranean Area, Vannucci and Gasperini, 2004). Such data have been used when they were the only available ones, thus for the relevant events occurred before the digital era of seismological data, as for instance the 1968 Belice (Sicily) earthquakes. In a few cases,

multiple focal mechanisms are available for a single event. To choose among them we applied the quality evaluation given in the EMMA Database selecting the so-called “preferred” solutions.

However, for two great events of the past century, the 1905 M6.9 in Calabria and the 1915 M6.9 in the Southern Apennines, several first arrival focal mechanisms available in the EMMA Database are available, unfortunately of low quality and different from one to another, indicating a different tectonic style from that expected in the regions where they occurred. For both earthquakes, none of the “preferred” nearly strike-slip solutions was considered reliable enough because the strike slip kinematic seems far to be compatible with the crustal tectonic style of the Southern Apennines and Calabria regions, usually described as extensional (e.g. D’Agostino et al., 2011).

Considering the high magnitude of these events and the aim of this study, we decided to look for different data to reconstruct their focal mechanisms. To do so we took into account the following statements: 1) first arrival focal mechanisms are often different from seismic moment tensor focal mechanisms (see the astonishing example of the M 6.0 Amatrice earthquake, Central Italy, August 24 2016 of Figure 2 in Marchetti et al., 2016); 2) first arrival focal mechanisms represent the initial fault slip, while seismic moment tensors describe the entire seismic source, which in turn is considered the most representative indicator of the tectonic style dominating the epicentral region.

Our attention thus went to Quaternary tectonics information in the DISS database (DISS Working Group, 2018), according to which the seismogenic sources of both events are described as pure extensional, based on geological studies (e.g. Loreto et al., 2013 for the 1905 Calabria earthquake; Galadini and Galli, 1999 for the 1915 earthquake). Thus, for the 1905 earthquake we used a seismic moment tensor reconstructed using the strike, dip and rake given in the seismogenic source ITIS139, Sant’Eufemia Individual Source, and for the 1915 those given in the ITIS002, Fucino Basin Individual Source. It is worth noting that from DISS we exported only the strike, slip and rake reported in the parameters lists, while for magnitude and seismic moment we kept those from the “preferred” solution in the EMMA database, because determined with seismological recordings, as all other similar data of our dataset.

The final database (Figure 1 and Table S2 in the Supplementary Material) includes nearly 1000 focal mechanisms for crustal earthquakes, representative of about 100 years of seismicity of the Italian peninsula and surrounding areas.

We are aware that for some regions the possible largest earthquake could be not represented in the available observations. Looking for the prevailing style-of-faulting, we needed information on the focal mechanism of events, which of course do not exist for great earthquakes of the past. This lack of knowledge should be taken into account together with other uncertainties when the results of this work will be used in hazard model computations, as well as it is done for data from historical catalogs, where it is known that ancient big earthquakes may lack. By the way, considering how long geological process last, we assume that where we have focal mechanisms for recent events coherent with geological structures, they may be considered representative of historical earthquakes, too.

For assessing seismic hazard, one of the main input element when adopting the classic Cornell (1968) approach is the seismic sources model, defined as areas with homogeneous characteristics in terms of seismicity, maximum magnitude, prevalent rupture and so on. Meletti et al. (2019) released a new model (ZS16) that represents the update of the model ZS9 (Meletti et al., 2008) adopted by the current reference seismic hazard model of Italy

(Stucchi et al., 2011). ZS16 is based on the same seismotectonic model used for designing ZS09, but many new data available for the study area (earthquake catalog and fault database among others) allowed a better definition of the boundary of each seismic source zone (Figure 2).

To identify the nodal planes of expected seismicity, representative for each of the 50 seismic source zones of the Seismogenic Area-based Model ZS16 (Meletti et al., 2019), we started applying the traditional Kostrov's method (Kostrov, 1974) for which the sum of the moment tensor elements M_{ij} is taken for all of the N earthquakes located within the volume V , obtaining a cumulative seismic moment tensor. This method can be applied to every volume for which earthquake moment tensors are available, that in our study means 41 of the 50 source areas (Table 1). In 5 of the remaining 9 areas, the summation cannot be done because they do not include any seismic event with magnitude greater or equal than $M 4.5$, while the other 4 areas have only one earthquake within the considered magnitude range.

Methods

Looking at the depth distribution of the Italian seismicity (Figure 1), it becomes immediately evident that the use of the same seismogenic thickness (the thickness of volume V within which the summation is done) along the entire peninsula is not appropriate. At first, we computed the cumulative seismic moment tensor for each zone with 10, 20 and 30 km of seismogenic layer thicknesses (e.g., for 20 km see Figure 2). Comparing the results of the three different computations, we obtained the following information:

- 20 km of seismogenic thickness is a coherent value for the 90% of the source areas (Table 1);
- in some zones the most representative seismicity is deeper, thus we used a thickness of 40 km to ensure the inclusion of all crustal seismicity (Table 1);
- in some other zones, completely different cumulative moment tensors are obtained using different seismogenic thicknesses. An example is given by the zone n. 19, in the Northern Apennines, where a seismogenic layer of 10 km only shows a purely extensional cumulative seismic moment tensor (Figure 3), while a layer of 20 km of thickness produces a thrust focal mechanism. We defined this behavior as a "tectonic layering" and, consequently, for similar situations we computed a summation over two different layers, with thickness depending on the local seismicity distribution with depth (Table 1).

We then followed these observations to define the volume used to compute all cumulative focal mechanisms; all values applied are reported in Table 1.

Several ground motion prediction equations include the "style-of-faulting" as a possible

variable (e.g. Bindi et al., 2011; Akkar et al., 2014; Bindi et al., 2014) and the modern seismic hazard softwares (e.g. OpenQuake Engine, Pagani et al., 2014) need the prevalent fault geometry of the expected ruptures to be used for the source definition. However, because the style-of-faulting impacts the PSHA in an area, it is important to define when the calculated style-of-faulting can be considered robust and representative of the kinematics of a region.

We started firstly applying a traditional Kostrov's method (Kostrov, 1974), in which the sum of the moment tensor elements M_{ij} is taken for all of the N_{ev} earthquakes located within the volume V , obtaining a cumulative seismic moment tensor representative of the seismic deformation occurred within V . This method can be applied to every volume, i.e. each seismic zone, for which earthquake moment tensors are available, that in our study means 41 of the 50 source areas (Table 1). In 5 of the remaining 9 areas, the summation cannot be done because no events with $M \geq 4.5$ are present, while the other 4 areas have only one earthquake within the considered magnitude range (Table 1).

A sensitive parameter is the depth of seismogenic layer we use in the summation for each zone. We already have indications from the values attributed to ZS16 seismic zones, but we also know that in some regions a change in the tectonic style with depth may occur, so we perform one test to find the most appropriate values.

We calculated the cumulative seismic moment tensors assuming different thicknesses of the volume V , equal for all zones, respectively of 10, 20 and 30 km (an example in Figure 2). Comparing the results, we observed that in some zones the cumulative moment tensors are different when calculated using different thickness. An example is given by zone n. 19 in the Northern Apennines, where a seismogenic layer of 10 km of thickness shows a purely extensional cumulative seismic moment tensor (Figure 3), while a summation over a layer of 20 km produces a transpressive focal mechanism. The distribution with depth of focal mechanism style of this part of the Apennines in fact shows a prevailing presence of extensional earthquakes in the shallower part of the crust while, moving E-NE, beneath normal sources, reverse and strike slip focal mechanisms are the most frequent (see Section in Figure 3). We defined schematically this behavior as a "tectonic layering", and where we detected it, in the three seismic zones n. 19, 20 and 25, we proceed with a summation over two different layers, with thickness depending on the local seismicity distribution with depth (Table 1). For all the other zones, we used a 40 km thickness for conservative reasons to make sure the inclusion of all selected seismic events in our computation.

These summation tests allowed also to investigate if the summed solutions were representative of the kinematics of each zone, and how the input dataset influences the robustness of the results. When the cumulative moment tensors were obtained summing data for $N_{ev} \geq 3$ and the input dataset was homogeneous as concerns the tectonic style, the results were consistent with the tectonics of the region and thus considered representative (red focal mechanisms in Figure 2). A good example is given by the Eastern Alpine region, where for seismic zones 1, 2 and 3, reverse and strike-slip cumulative focal mechanisms well reflect the compressive active tectonic of Southern Alps and the strike-slip deformation which prevails to the east in the Dinaric chain. On the contrary, when the cumulative moment tensor was the sum of three or less moment tensors (yellow focal mechanisms in Figure 2), or it was obtained with more than three earthquakes, but with the summation of a heterogeneous dataset (light blue focal mechanisms in Figure 2), i.e. several focal mechanisms with different tectonic styles and/or very different directions of strike, dip and

rake, we considered the results insufficiently representative. This last case occurs mainly in seismic zones characterized by small to moderate magnitude earthquakes, or including seismotectonic structures with different orientations. An example is the area source n. 11, which contains part of western Alps and the western Po Plain (Figure 2), where most of available focal mechanisms are strike slip, but with very different and scattered directions of the focal planes.

To reduce the amount of such unreliable results, that affect nearly half of the seismic zones, we implemented the following methodology. In each seismic zone we splitted the entire dataset in the three main tectonic styles, following the rake-based criteria given in Akkar et al. (2014) which attribute each focal mechanism to a specific kinematics, reverse, normal or strike-slip. In particular, normal solutions have a rake between -135° and -45° , reverse solutions between 45° and 135° , other rake values are classified as strike slip.

We then applied the Kostrov summation over each homogenous — from the tectonic point of view — group of moment tensors having more than one earthquake. In Table 1 the results for each zone are reported (cumulative M_0 , strike, dip and rake of the cumulative focal mechanism for each tectonic style).

We computed also the dispersion of the P-, T- and B- axes of the input focal mechanisms with respect to the position of the P-, T- and B- axes of the cumulative moment tensor (Table 2). For example, as reported in Figure 4, in the source area n. 9 we have 7 input data; we computed the angular distance between the P- T- and B- axes (red and blue points in Figure 4a) and the axes of the cumulative focal mechanism (green symbols in Figure 4a). The three median values of the angular distances of the three axes are a measure of how much dispersed and heterogeneous are the input data, and consequently of the robustness of the obtained nodal plane distribution. The three median values are then used as a weighting factor for defining the final style of faulting for each zone.

The main purpose of this study is to identify, when possible, the prevailing tectonic style and a representative seismic source in each seismogenic area to be used in the seismic hazard modelling, for the choice of coefficients of the ground motion prediction equations and for the kinematics of the seismogenic sources. Indeed, several ground motion prediction equations include “style of faulting” as a possible variable (e.g. Bindi et al., 2011; Akkar et al., 2014; Bindi et al., 2014) and modern softwares for seismic hazard computation (e.g. OpenQuake Engine, Pagani et al., 2014) need the definition of the prevalent fault geometry of the expected ruptures to be used for the source definition. Cumulative moment tensors may certainly be representative, but it is important to define when they can be considered robust enough.

To identify the representative style-of-faulting for each source zone, we used a procedure based on the following parameters:

- N_{ev} , the number of available focal mechanisms for each zone and for each tectonic style.
- M_{0sum} , the seismic moment obtained from the summation for each zone and tectonic style; in particular its percentage with respect to the M_{0Total} , the total seismic moment for each seismic zone independently by the tectonic style (Table 3).
- the median of the angular distance between P-, T-, B- axes (Table 2), as a measure

of data input dispersion.

First of all, we investigated if the summed solutions within each zone and the input dataset of focal mechanisms were coherent. In Figure 2, red focal mechanisms represent a coherent result, that means that the cumulative moment tensor was obtained with data of more than three earthquakes, and that the input dataset was homogeneous as concerns the tectonic style. Yellow focal mechanisms, on the contrary, cannot be considered for our analysis because they were obtained summing three or less moment tensors. Light blue focal mechanisms are obtained with more than three earthquakes, but with the summation of a heterogeneous dataset, i.e. several focal mechanisms with different tectonic styles and/or very different directions of strike, dip and rake. This last case occurs mainly in seismic zones characterized by small to moderate magnitude earthquakes, or including seismotectonic structures with different orientations. An example is the area source n. 11, which contains part of western Alps and the western Po Plain (Figure 2).

The value of these parameters has been used to apply the following decision-making process, also sketched in Figure 5:

o avoid the problems related to the heterogeneity of the dataset, we implemented the procedure as follows. In each seismic zone we splitted the entire input dataset in the three main tectonic styles, following the criteria given in Akkar et al. (2014) for thrust, normal and strike-slip earthquakes, and we applied the summation over each homogenous — from the tectonic point of view — group of moment tensors having more than one earthquake. In Table 2 the results for each zone (cumulative M_0 , strike, slip and rake of the cumulative focal mechanism for each tectonic style) are reported.

a) in areas where no focal planes at all were available, we parameterized the less informative solution, given by a equal contributions of normal, reverse and strike-slip tectonic styles, and by adopting a uniform distribution of geometries (strike and dip) in the space, defining a 100% random source;

b) if more than one event of the same tectonic style is located in an area, we identified the nodal planes and their contributions in terms of seismic moment M_0 . As a first step we summed the seismic moment tensors to obtain M_{0sum} and a cumulative moment tensor, then we apply the following criteria:

- if M_{0sum} for a particular tectonic style is lower than the 10% of M_{0Total} of the zone, we do not take into account that tectonic style in the final solution. For example, in the zone n. 39, the strike-slip component is not included in the final result (Tables 1 and 3);
- if M_{0sum} of a single tectonic style is greater than the 10% of M_{0Total} of the zone, but the number of summed earthquakes is lower than 3, we kept this tectonic style in the final seismic source by adopting a uniform distribution of geometries (strike-dip) in the space with a fixed rake, also defined as a random component. An example is the zone n. 12 (Tables 1 and 3), where the compressive contribution is included, defined as TFRandom, but modelled without preferred fault planes;
- for each tectonic style of the zones with a contribution in M_{0sum} greater than the 10% of M_{0Total} and obtained with a number of earthquakes greater than 2, we measure the dispersion of the P-, T- and B- axes of the input focal mechanisms with respect to those of the cumulative moment tensor: if 2 or more of the three axes have the

median of the angular differences greater than 30° (Table 2), we include this tectonic style, but adopting a uniform distribution of geometries (random strike and dip) in the space with a fixed rake. An example is given by zone n. 9 where all data are strike-slip, but the analysis of P-, T- and B- axes distributions shows a dispersion larger than 30° for two of three axes (Figure 4) and the final style-of-faulting is 100% strike-slip random;

- if the M_{0sum} of a single tectonic style is greater than the 10% of the M_{0Total} , obtained with a number of events greater than 2, and with the maximum of the median of the angular distances of P-, T- and B- axes greater than 30°, it contributes to the final solution proportionally to its percentage with respect to the M_{0Total} . Moreover, the final focal mechanism is given by the cumulative one obtained by the Kostrov summation of available moment tensors of the single tectonic styles. An example is given by zone n. 43, where the final style-of-faulting is represented by a 45% of reverse source and 55% of a strike-slip; strike, dip and rake values reported in Table 3 for these final solutions originate from the cumulative moment tensors obtained summing respectively reverse and strike-slip input focal mechanisms.

Applying this decision making process to all seismic zones, we defined an expected style-of-faulting for all of them, reported in Table 3 and in Figure 6.

To take into account the complete characteristics of the input dataset with respect to the cumulative results, in particular the homogeneity of the resulting summed data with respect to the input data, we computed the dispersion of the P-, T- and B- axes of focal mechanisms in each sub-dataset and then compared it with the directions of the P-, T- and B- axes of the cumulative moment tensor. This comparison has been done for the three tectonic styles in each seismic zone and has been used as one of the criteria for the expected source tectonic style evaluation (Figure 4):

To identify the representative distribution of nodal planes for each source zone, subsequently for each tectonic style, we used the following approach:

a) in areas where no focal planes at all were available, we parameterized the less informative solution, given by equal contributions of normal, reverse and strike-slip tectonic styles, and by adopting a uniform distribution of geometries (strike and dip) in the space;

b) if more than one event of the same tectonic style is located in an area, we identified nodal planes and their contributions. As a first step we summed M_0 and moment tensors of the events to obtain a total M_0 and a cumulative moment tensor, then:

- if the sum of M_0 for a particular tectonic style is lower than the 10% of the total M_0 of the zone, we removed the contribution of that tectonic style from the final solutions of nodal planes (for example: zone n. 39 in Tables 2, where the strike-slip component is not included in the final result reported in Table 1);
- if the contribution of the sum of M_0 of a single tectonic style is greater than the 10% of the total M_0 of the zone, but the number of summed earthquakes is lower than 3, we

kept this tectonic style in the final seismic source by adopting a uniform distribution of geometries (strike-dip) in the space with a fixed rake. An example is the zone n. 12 (Tables 1 and 2), where the compressive contribution is included, but modelled without preferred fault planes;

- for each tectonic style of the zones with a contribution in M_0 greater than the 10% obtained with a number of earthquakes greater than 2, we performed a dispersion analyses of the P-, T- and B- axes of the input focal mechanisms with respect to those of the cumulative moment tensor: if at least 2 axes have a dispersion greater than 30° , we included the tectonic style, but adopting a uniform distribution of geometries (strike-dip) in the space with a fixed rake. An example is given by zone n.9 where all data are strike-slip, but the analysis of the distributions has underlined a dispersion larger than 30° (Figure 4);
- the contributions of the summed M_0 of a tectonic style, when they are greater than the 10% of the total M_0 , are used to weight the corresponding nodal planes solutions determining the percentage of each tectonic style in the final expected one.

Results

On the basis of these criteria, the expected tectonic style in each seismic zone has been defined as reported in Table 1.

In Figure 6 and Table 3 the results of the applied decision making process are shown. The variety of symbols and colors of Figure 6 represents the complexity of the seismotectonics of the Italian peninsula, and the attempt we made at taking all of them into account, encountering all possible cases between the 100% single tectonic style source to the 100% random source.

Tectonic Styles and expected focal solutions in the ZS16 Seismogenic Model

In only 15 zones the resulting focal solution is 100% of a single tectonic style, and often this occurs where great earthquakes are located, as in zone n. 33 which includes the 1980 Irpinia M 6.9 event. On the other hand, in 10 seismic areas the final source is 100% random, due to the lack or scarcity of seismic events with $M \geq 4.5$, as for instance the zones n. 27 or 31 along the Tyrrhenian coast or the n. 37 and 38, offshore southern PugliaFigure 5 and Tables 1 and 2, the main results are shown. In 15 zones the resulting focal solution is 100% of a single tectonic style, while in several zones there is a partitioning between more than one tectonic style, with weights defined by the contributions of cumulative seismic moment M_0 . For instance, in the seismic zone n. 30 (Central Adriatic Sea), the tectonic style of the expected seismic source is 80% compressive and 20% strike-slip, giving up the 5% of normal style because lower to the 10% threshold. In some zones, the expected source tectonic style we determined may have a percentage of uniform distribution of geometries (strike-dip) in the space (defined for instance as NFr and, TFrand or SSrand in Table1).

When a tectonic style can be used at least as a constraint, a fixed rake is adopted. In the seismic zone n. 29 (Chieti-Pescara) we obtained a source composed by 80% of compressive component and 20% of *random* strike-slip, i.e. strike-slip mechanism with uniformly distributed value for strike and dip and a fixed rake. In other zones, the final result is given by different percentages of more than one tectonic style, all random. For instance, in zone n. 40, the Ionian Sea side of the Calabria region, the final result is a combination of 15% extensional random and 85% strike-slip random. These kinds of results are mainly due to the heterogeneity of the input dataset. When a tectonic style is poorly represented, i.e. the number of focal mechanisms to be summed is lower or equal to 3, the summation may be used anyway to parameterize the expected source tectonic style. For instance, in the NW of Italy, in the seismic zones n. 9, 10 and 11 (Table 1), the seismic source that may be applied in the hazard modelling is a uniform distribution of strike-slip geometries, because this is the tectonic style that prevails, but with an undetermined strike direction.

For 3 zones, where a tectonic layering has been identified, the expected source tectonic style is defined for both shallow and deep seismicity (represented in Figure 5 with focal mechanisms with a grey background or with circles with a grey border). The seismic zone n. 19s, for instance, has a shallow final source 50% extensional, 35% strike-slip and 15% compressive random; the deep final seismic source (19d in Table 1, hypocentral depth between 15 and 40 km) is 100% thrust.

In several zones the final style-of-faulting is a partitioning between more than one tectonic style, with contributions defined by the percentage of the seismic moment M_{0sum} of each tectonic style. For instance, in the seismic zone n. 30 (Central Adriatic Sea), the tectonic style of the final seismic source is 80% compressive and 20% strike-slip. A 5% of normal style is excluded because it does not reach the 10% threshold (Figure 5).

In some zones, the final style-of-faulting has a percentage of uniform distribution of geometries (strike-dip) in the space, that for the sake of simplicity we defined as a random component, namely NFRandom, TFRandom or SSRandom (Table 3). This means that when a tectonic style can be used only as a constraint, a proper fix rake is adopted. In the seismic area n. 29 we defined a final style-of-faulting composed by 80% of reverse tectonic type and 20% of random strike-slip, i.e. a strike-slip mechanism with uniformly distributed value for strike and dip and a fixed rake.

Another case is represented by zones where the final source is given by different percentages of more than one tectonic style, all random. For instance, in zone n. 40, the Ionian Sea side of the Calabria region, the final result is a combination of 15% extensional random and 85% strike-slip random. These kinds of results occur mainly where the input dataset shows a large dispersion and heterogeneity in input focal plane directions. For instance, in the NW of Italy, in the seismic zones n. 9, 10 and 11 (Table 3), the final style-of-faulting we propose is a uniform distribution of strike-slip geometries, derived from several earthquakes located in the area, mostly strike-slip, but without any prevailing direction for the strike of focal planes.

A tectonic layering has been identified in three seismic zones, n.19, 20 and 25, so we defined a style-of-faulting for both a shallow and a deep seismogenic layer (the latter, represented in Figure 6 with focal mechanisms with a grey background or with circles with

darker colours). The seismic zone n. 19s, for instance, has a final source composed by a 50% normal, 35% strike-slip and 15% compressive random; the final result for the deep layer (19d in Table 3, hypocentral depth between 15 and 40 km) is a 100% reverse style-of-faulting.

Discussion and Conclusions

Discussion

We defined the tectonic style of possible expected relevant earthquakes for each seismic zone of the Seismogenic Area-based Model ZS16 (Meletti et al., 2019) on the basis of the availability and robustness of input data. Our results derive from a cascade criteria approach aimed at retrieving all the possible information on ~100 years of seismicity in Italy. Our final expected source tectonic styles are reported in Tables 1 and 2, and in Figure 5.

The reliability of our analysis is confirmed also by the comparison with results given by Roselli et al. (2017), which used a different approach. Roselli et al. (2017) smoothed their dataset over a regular 0.1° grid and did not take into account the possible variability of the prevailing tectonic styles with depth. From a qualitative point of view, we observed a general agreement between the results, with major differences in the resulting tectonic styles along the boundary between areas that in Roselli et al. (2017) are characterized by lateral changes of tectonic regimes. It is worth noting that these are the regions where we used a 3D approach, including the possible change of tectonic style with depth, as for instance in the Northern Apennines (zone n. 19, Table 1).

To further evaluate if and how our results are reliable indicators of the tectonic style of expected earthquakes we compared them with recent earthquakes occurred in Italy. Indeed, the input dataset includes only events occurred before the end of 2015. So, all the seismicity recorded more recently in Italy, including the 2016-2017 Central Italy seismic sequence, may be used for a comparison test. Selecting from the INGV bulletin (<http://cnt.rm.ingv.it/events>) all shallow earthquakes (within 40 km of hypocentral depth) with M from 4.5 occurred between January 2016 and August 2019, we obtain the list of earthquakes reported in Table 3. We also included 4 events with M from 4.2 to 4.4 to increase the casuistry. For all these recent earthquakes, the corresponding seismic moment tensors have been extracted from the European Mediterranean RCMT Catalog (Figure 6, <https://doi.org/10.13127/rcmt/euromed>). For earthquakes belonging to the Central Italy seismic sequence, we selected the greatest ones only: the August 24, 2016, Mw 6.0, the October 30, Mw 6.5 and the January 18, 2017, Mw 5.5. Starting from them, all with an extensional moment tensor, it is evident the agreement with the tectonic style defined for the seismic zone n. 24, where the expected source tectonic style we obtained is 100% normal (Figure 6, map top right). Following in the comparison, another correspondence is found in the Northern Apennines, where an event located below 15 km of hypocentral depth (Figure

6, event n.6 in the top left map and in Table 3), thus in the lower layer for the seismic zone n.19, shows a good similarity with what we expected. A great agreement is found for the event located at the border of the seismic zone n. 21, where expected and occurred seismic sources are both pure thrust (Figure 6, top left, events n. 12 in Table 3). The same can be said for the two strike-slip events occurred in the summer of 2018 in the seismic zone n.34, both showing a strong coherence with the expected tectonic style (Figure 6, events n. 8 and 9 in the top right map and in Table 3). In Sicily, all recent earthquakes show a strike-slip focal mechanism, in agreement with our results (Figure 6, map below).

This similarity between the seismic moment tensors of recent earthquakes and the final solution we defined for each area source is an important support to the reliability of our results. Moreover, the seismic events occurred in the last years positively tested several of the 50 seismic zones of the Seismogenic Area-based Model we used. In addition, recent earthquakes positively tested also the change of the prevailing tectonic regime with depth, as in the Northern Apennines.

We propose a set of criteria to select focal mechanisms for the definition of the style-of-faulting in area source models, and we apply them to the ZS16 seismotectonic zoning (Meletti et al., 2019). Results are shown in figure 6 and listed in Table 3. We are confident in our results for several reasons.

The first is that the style-of-faulting defined for each zone using our decision-making process are strongly in agreement with other geological (DISS Working Group, 2018) and geodetic data (Serpelloni et al., 2005; D'Agostino et al., 2011). For instance, the normal tectonics that characterizes the Apennines is confirmed in all the seismic zones that concern the highest part of the belt. The normal tectonic style changes to compressive and/or strike-slip moving toward the Adriatic side or going at depth; two of the three zones where a variation of the tectonic style with depth has been detected, show a prevailing extensional regime at shallow depth and a deeper reverse and/or strike-slip tectonic type. For the Alpine region, the western part of the belt presents more uncertain results due to the characteristics of the seismicity, usually characterized by small to moderate magnitude; in the Eastern Alps our results are completely in agreement with the active deformation field, with compressive to transpressive tectonics of the Southern Alps and Dinarides.

A second reason that supports the reliability of our analysis is the comparison with the results given by Roselli et al. (2017), who used a different approach. Roselli et al. (2017) smoothed their dataset over a regular 0.1° grid and did not take into account the possible variability of the prevailing tectonic styles with depth. From a qualitative point of view, we observed a general agreement between our results, with major differences along the boundary between areas that in Roselli et al. (2017) are characterized by lateral changes of tectonic regimes. It is worth noting that these are the regions where we detected a variation of the style-of-faulting with depth and so where we used a 3D approach. For instance in the Northern Apennines we obtain different, even opposite, style-of-faulting at different depths, as in zone n. 19, where the shallow solution is mainly normal type while at depth is a reverse type. However, at the same time lateral variation in our results is smoothed and not related

to the presence of a boundary, like the one between two seismic zones. Modelling the earthquake occurrence in this region, the definition of the hypocentral depth makes the difference; if we model a seismic event deeper than 15 km beneath zones 19 or 20, we should assume a mainly reverse style-of-faulting, and so a GMPE different from the one to be used if the earthquake was shallower, i.e with a normal style-of-faulting.

To further evaluate when our results are reliable indicators of the style-of-faulting of expected earthquakes we compared them with recent earthquakes. Indeed, the input dataset includes only events before 2015. So, all the seismicity recorded afterwards, including the 2016-2017 Central Italy seismic sequence, can be used for a comparison test. Selecting from the INGV Italian Seismological Instrumental and Parametric Data-Base (ISIDe Working Group, 2007) all shallow earthquakes (within 40 km of hypocentral depth) with $M \geq 4.5$ occurred between January 2016 and August 2019, we obtain the list of earthquakes reported in Table 4. We also included 4 events with M from 4.2 to 4.4 to increase the case studies. For all these recent earthquakes, the corresponding seismic moment tensors have been extracted from the European Mediterranean RCMT Catalog (Figure 7). For earthquakes belonging to the Central Italy seismic sequence, we selected the largest ones only: the August 24, 2016, Mw 6.0, the October 30, Mw 6.5 and the January 18, 2017, Mw 5.5. Starting from them, all with an extensional moment tensor, it is evident the agreement with the style-of-faulting defined for the seismic zone n. 24, where the expected source tectonic style is 100% normal (Figure 7C). Proceeding in the comparison, another correspondence is found in the Northern Apennines, where an event located below 15 km of hypocentral depth (Figure 7A, event n.6 in Table 4), thus in the lower layer of seismic zone n.19, shows a good similarity with the style-of-faulting defined for the area. A good agreement is found for the event located at the border of the seismic zone n. 21, where expected and observed style-of-faulting are both pure reverse (Figure 7A, event n. 12 in Table 4). The same applies to the two strike-slip events occurred in the summer of 2018 in the seismic zone n.34, both showing a strong coherence with the expected style-of-faulting (Figure 7C, events n. 8 and 9 in Table 4). In Sicily, all recent earthquakes show a strike-slip focal mechanism, in agreement with our results (Figure 7B, map below). In conclusion, recent earthquakes positively test our results, also in sources obtained following the choice to allow a 3D approach where necessary, as in the Northern Apennines.

Conclusions

The methodology we proposed to calculate the style-of-faulting in a seismic zone model is based on the selection of input data (focal mechanisms) aimed to ensure: (i) representativeness of the observed kinematics expected to occur in the future; (ii) summation of focal mechanisms representative of similar style-of-faulting; (iii) the control of the dispersion of the nodal planes before their summation with respect to the cumulative one. Finally, the here described procedure can be exported to any area source based model, as it represents a data-driven approach, with subjectivity restrained to define threshold for dispersions of the input focal mechanisms.

Ultimately, we defined the tectonic style-of-faulting of possible expected earthquakes for each seismic zone of the seismogenic area source model ZS16 (Meletti et al., 2019).

In Figure 6, the final results map, the various symbols we had to use reflect all the different situations we detected and mirror the seismotectonic complexities we took into account even

on a simplified seismic zones model. On a general view, in the Alps a compressive regime is found in the eastern part of the belt (zones n. 1, 2, 3), mixed in a different percentage with a strike-slip style-of-faulting moving toward the Dinaric chain to east. The rest of the Alps shows examples of all the possible style-of-faultings with also all the different percentages of random sources, sometime 100% random (e.g. zones n. 6, 8, 14), sometime a combination of different amounts of single tectonic style random sources (e.g. zone n. 11), and this is due mainly because Western and Central Alps are characterised by a small to moderate seismicity only.

In our results the expected normal regime dominating the Apennines is confirmed, all along the watershed (zones. n. 18, 19, 24, 33, 39, 45), following the typical tectonic style of the seismic sequences occurred in this narrow zone in the last tens of years, i.e. from north to south the 1997-1998 Umbria Marche, the 2016-2017 Central Italy, the 2009 L'Aquila and the 1980 Irpinia. In the outer part of the Apennines the style-of-faulting changes with depth and moving to east, to a reverse regime, sometime mixed with a strike-slip style, as in the zones n. 21, 26, 29, 34 and 36. The 3D approach we applied, allowed to detect the transition from normal to reverse with depth along the Northern and Central Apennines and to solve the abruptness of this transition given by a 2D approach only.

Along the peninsula, few seismic zones have a final 100% random source result and this occurs where the seismicity is really scarce and with small to moderate earthquakes (zones n. 22, 27, 28, 31, 37 and 38).

The seismic zones where however the strike-slip style of faulting mainly dominates are in Eastern Sicily, from the Aeolian Islands through the Etna volcano toward south up to the Iblei mountains (zones n. 44, 49, 48); this is not surprising considering that this N-S narrow band is interpreted as the transfer zone between the Calabrian arc subduction system and the Sicily continental environment.

The robustness of these results is confirmed by their correspondence with the geological models and by the good comparison made with the most recent earthquakes occurred in Italy, independently from their magnitudes. Finally, these results are in use in the recent elaboration of a new seismic hazard model for Italy.

Acknowledgement

This paper describes one of the many products released in the framework of the activities of INGV Seismic Hazard Center (Centro Pericolosità Sismica, CPS) for producing MPS19, the new seismic hazard model of Italy. This study has benefited from funding provided by the Italian Presidenza del Consiglio dei Ministri - Dipartimento della Protezione Civile (DPC). This paper does not necessarily represent DPC official opinion and policies. All maps have been plot using GMT mapping tool (Wessel & Smith, 1998; Figure 4a plot has been produced using FaultKin 7.7.4 (Marrett and Allmendinger, 1990; Allmendinger et al., 2012) Most figures were made using GMT software (Wessel and Smith, 1998).

Competing interests

The authors declare that they have no conflict of interest.

Data availability

The dataset of focal mechanisms used for this study is included in the Supplement (see below). All results and data used to obtain them are reported in Tables in the text

Supplementary Material

Table 1_Supplement — Dataset used in this study, gathering all seismic moment tensors

~~used in this work, including also single earthquake information.~~

Supplements

[Table 1_Supplement — Depth parameters used for ZS16 seismic zones.](#)

[Table 2_Supplement — Dataset used in this study, gathering all seismic moment tensors used in this work, including also single earthquake information.](#)

References

[Allmendinger, R. W., Cardozo, N., and Fisher, D., 2012, Structural geology algorithms: Vectors and tensors in structural geology: Cambridge University Press, 302 p.](#)

[Anzidei, M., Maramai, A. and Montone, P. \(eds\): The Emilia \(northern Italy\) seismic sequence of May-June, 2012: preliminary data and results, *Ann. of Geophysics*, 55, 4, 515-842, doi: 10.4401/ag-6232, 2012.](#)

[Akkar, S., M. A., Sandikkaya and J. J. Bommer: Empirical ground-motion models for point- and extended-source crustal earthquake scenarios in Europe and the Middle East, *Bull. Earthquake Eng.*, 12:359–387, 10.1007/s10518-013-9461-4, 201, 2014. Empirical ground-motion models for point- and extended-source crustal earthquake scenarios in Europe and the Middle East, *Bull. Earthquake Eng.*, 12:359–387, DOI 10.1007/s10518-013-9461-4.](#)

[Bernardi, F., Braunmiller, J., Kradolfer, U. and Giardini, D.: Automatic regional moment tensor inversion in the European-Mediterranean region, *Geophys. J. Int.*, 157, 703–716, 2004& Giardini, D., 2004. Automatic regional moment tensor inversion in the European-Mediterranean region, *Geophys. J. Int.*, 157, 703–716.](#)

[Bindi, D., Pacor, F., Luzi, L., Puglia, R., Massa, M., Ameri, G. and Paolucci, R.: Ground motion prediction equations derived from the Italian strong motion database, *Bull. Earthquake Eng.*, 9, 1899–1920, <https://doi.org/10.1007/s10518-011-9313-z>, 2011D'Agostino, N., D'Anastasio, E., Gervasi, A., Guerra, I., Nedimović, M.R., Seeber, L., Steckler, M., 2011. Forearc extension and slow rollback of the Calabria Arc from GPS measurements. *Geophys. Res. Lett.*, 38, 117304, <http://dx.doi.org/10.1029/2011GL048270>.](#)

[Bindi, D., Massa, M., Luzi, L., Ameri, G., Pacor, F., Puglia, R. and Augliera, P.: Pan-European ground-motion prediction equations for the average horizontal component of PGA, PGV, and 5 %-damped PSA at spectral periods up to 3.0 s using the RESORCE dataset. *Bull Earthquake Eng* 12, 391–430, <https://doi.org/10.1007/s10518-013-9525-5>, 2014. DISS Working Group \(2018\). Database of Individual Seismogenic Sources \(DISS\), Version 3.2.1: A compilation of potential sources for earthquakes larger than M 5.5 in Italy and surrounding areas. <http://diss.rm.ingv.it/diss/>, Istituto Nazionale di Geofisica e Vulcanologia; DOI:10.6092/INGV.IT-DISS3.2.1.](#)

[Bommer, J.J., Douglas, J. and Strasser, F.O.: Style-of-Faulting in Ground-Motion Prediction Equations, *Bulletin of Earthquake Engineering* 1, 171–203, <https://doi.org/10.1023/A:1026323123154>, 2003.](#)

[Dziewonski, A. M., T. A. Chou and J. H. Woodhouse, Determination of earthquake source parameters from waveform data for studies of global and regional seismicity, *J. Geophys. Res.*, 86, 2825–2852, 1981. doi:10.1029/JB086iB04p02825](#)

CMT Italian Dataset, <http://rcmt2.bo.ingv.it/Italydataset.html>, doi:10.13127/rcmt/italy, last access: 15 July 2020 Ekström, G., M. Nettles, and A. M. Dziewonski, The global CMT project 2004–2010: Centroid-moment tensors for 13,017 earthquakes, *Phys. Earth Planet. Inter.*, 200–201, 1–9, 2012. doi:10.1016/j.pepi.2012.04.002.

Chiarabba, C., De Gori, P., Cattaneo, M., Spallarossa, D. and Segou, M.: Faults geometry and the role of fluids in the 2016–2017 Central Italy seismic sequence, *Geophysical Research Letters*, 45, 6963– 6971, <https://doi.org/10.1029/2018GL077485>, 2018 Galadini, F., and P. Galli 1999 The Holocene paleo-earthquakes on the 1915 Avezzano earthquake faults (central Italy): implications for active tectonics in the central Apennines. *Tectonophysics*, 308, 143–170.

D'Agostino, N., D'Anastasio, E., Gervasi, A., Guerra, I., Nedimović, M.R., Seeber, L. and Steckler, M.: Forearc extension and slow rollback of the Calabria Arc from GPS measurements, *Geophys. Res. Lett.*, 38, 117304, <http://dx.doi.org/10.1029/2011GL048270>, 2011 Marchetti et al., 2016. The Italian Seismic Bulletin: strategies, revised pickings and locations of the central Italy seismic sequence, *Ann. Geophysics*, 59, DOI: 10.4401/ag—7169.

DISS Working Group: Database of Individual Seismogenic Sources (DISS), Version 3.2.1: A compilation of potential sources for earthquakes larger than M 5.5 in Italy and surrounding areas, <http://diss.rm.ingv.it/diss/>, Istituto Nazionale di Geofisica e Vulcanologia, 10.6092/INGV.IT-DISS3.2.1, 2018, last access: 15 July 2020 Meletti G., Visini F., D'Amico V., Pace B., Rovida A., 2019. The seismicity model for Italy MA4. Internal report Seismic Hazard Center.

Dziewonski, A. M., Chou, T.-A. and Woodhouse, J. H.: Determination of earthquake source parameters from waveform data for studies of global and regional seismicity, *J. Geophys. Res.*, 86, 2825–2852, doi: 10.1029/JB086iB04p02825, 1981 Meletti, G., Marzocchi, W. & MPS16 Working Group, 2017. The 2016 Italian seismic hazard model, in Proc. 16th World Conference on Earthquake Engineering, Santiago de Chile, January 9–13, 747, S-P1463070033.

Ekström, G., Nettles, M. and Dziewonski, A. M.: The global CMT project 2004-2010: Centroid-moment tensors for 13,017 earthquakes, *Phys. Earth Planet. Inter.*, 200–201, 1–9, <https://www.globalcmt.org>, doi:10.1016/j.pepi.2012.04.002, 2012 Kostrov, V. V., 1974. Seismic moment and energy of earthquakes and seismic flow of rocks, *Izv. Acad. Sci. USSR, Phys. Solid Earth*, 1, 23–40.

European Mediterranean RCMT Catalog, <http://www.bo.ingv.it/RCMT>, doi:10.13127/rcmt/euromed, last access: 15 July 2020.

Pondrelli, S., A. Morelli, G. Ekström, S. Mazza, E. Boschi, and A. M. Dziewonski, 2002, European-Mediterranean regional centroid-moment tensors: 1997–2000, *Phys. Earth Planet. Int.*, 130, 71–101, 2002

Galadini, F. and P. Galli, P.: The Holocene paleo-earthquakes on the 1915 Avezzano earthquake faults (central Italy): implications for active tectonics in the central Apennines.

Tectonophysics, 308,143-170, 1999Pondrelli, S., S. Salimbeni, G. Ekström, A. Morelli, P. Gasperini and G. Vannucci, 2006, The Italian CMT dataset from 1977 to the present, Phys.-Earth Planet. Int., doi:10.1016/j.pepi.2006.07.008,159/3-4, pp. 286-303.

Gasperini, P., Lolli, B., and Vannucci, G.: Relative frequencies of seismic main shocks after strong shocks in Italy, Geophysical Journal International, 207, 1, 150–159, https://doi.org/10.1093/gji/ggw263, 2016Pondrelli S. and Salimbeni S., Regional Moment-Tensor Review: An Example from the European-Mediterranean Region. In Encyclopedia of Earthquake Engineering (pp. 1-15), http://link.springer.com/referenceworkentry/10.1007/978-3-642-36197-5_301-1, Springer Berlin Heidelberg, 2015.

ISIDe Working Group: Italian Seismological Instrumental and Parametric Database (ISIDe), Istituto Nazionale di Geofisica e Vulcanologia (INGV), https://doi.org/10.13127/ISIDE, 2007, last access: 15 July 2020Roselli, P., W. Marzocchi, M. T. Mariucci and P. Montone, 2017.- Earthquake focal mechanism forecasting in Italy for PSHA purposes. Geophys. J. Int., 212,-491–508, doi: 10.1093/gji/ggx383.

Loreto, M.F., Fracassi, U., Franzo, A., Del Negro, P., Zgur, F., and Facchin, L.: Approaching the seismogenic source of the Calabria 8 September 1905 earthquake: New geophysical, geological and biochemical data from the S. Eufemia Gulf (S Italy), Marine Geology, 343, 62-75, ISSN 0025-3227, https://doi.org/10.1016/j.margeo.2013.06.016, 2013Saul, J., Becker, J., Hanka, W. (2011): Global moment tensor computation at GFZ Potsdam, AGU 2011 Fall Meeting (San Francisco 2011).

Marchetti, A. et al.: The Italian Seismic Bulletin: strategies, revised pickings and locations of the central Italy seismic sequence, Ann. of Geophysics, 59, DOI: 10.4401/ag -7169, 2016Vannucci, G. Gasperini, P. 2004, The new release of the database of Earthquake Mechanisms of the Mediterranean Area (EMMA Version 2), Annals of Geophysics, Supplement to V. 47, N.1, 307-334.

Marrett, R. A., and Allmendinger, R. W.: Kinematic analysis of fault-slip data, J. of Structural Geology, v. 12, p. 973-986, 1990Wessel, P., and H.F. Smith (1998). New, improved version of 538 the generic mapping tools released, Eos Trans AGU, 539, 79-579;- doi:10.1029/98EO00426.

Meletti, C., Galadini, F., Valensise, G., Stucchi, M., Basili, R., Barba, S., Vannucci, G. and Boschi, E.: A seismic source model for the seismic hazard assessment of the Italian territory, Tectonophysics., 85-108,10.1016/j.tecto.2008.01.003, 2008.

Meletti, C., Visini, F., D'Amico, V., Pace, B. and Rovida, A.: The seismicity model for Italy MA4. Internal report Seismic Hazard Center, 2019.

TABLES

Meletti, C., Marzocchi, W. and MPS16 Working Group: The 2016 Italian seismic hazard model, in Proc. 16th World Conference on Earthquake Engineering, Santiago de Chile, January 9–13, 747, S-P1463070033, 2017 Table 1—Results of summation and analysis for all seismic zones in ZS16, numbers are in Figure 2. (NF= normal; SS= strike-slip; TF= thrust). If “rand” is included in the final source definition, that tectonic style is adopted as a uniform distribution of geometries (strike-dip) in the space with a fixed rake.

N.	Seismic Zone Name	Thickness (km)	Total n. of foc. mec.	Total M_0 (Dyn-cm)	%N F	%S S	%T F	Final Source Tectonic Style
1	Idria	0–40	9	3,94E+24	0	98	2	SS 100%
2	Slovenia	0–40	6	1,35E+24	0	87	13	SS 85% + TF 15%
3	Friuli	0–40	29	9,15E+25	0	11	89	TF 90% + SS 10%
4	Valtellina–Alto Adige	0–40	3	6,96E+23	0	79	21	SSrand 80% + TFrاند 20%
5	Innsbruck	0–40	1					
6	Grigioni	0–40	5	1,11E+24	90	10	0	NF 100%
7	Garda–Soncino	0–40	6	1,25E+24	10	52	38	SSrand 60% + TFrاند 40%
8	Montreux	0–40	1					
9	Vallese	0–40	7	9,10E+23	0	100	0	SSrand 100%
10	Western Alps	0–40	13	4,81E+24	7	93	0	SSrand 100%
11	Piemonte	0–40	10	1,98E+24	11	88	1	NFrاند 10% + SSrand 90%
12	Mantova–Verona	0–40	6	1,03E+24	0	76	24	SS 75% + TFrاند 25%
13	Pianura veneta	0–40	0					
14	Imperiese	0–40	4	5,87E+23	56	19	25	rand 100%
15	Mar-Ligure	0–40	6	1,42E+25	0	5	95	TF 100%
16	Tortona–Bobbio	0–40	11	1,17E+24	13	83	4	NFrاند 15% + SSrand 85%
17	Spezia–North of Tuscany	0–40	8	4,53E+23	27	68	5	SS 70% + NFrاند 30%
18	Lunigiana–Casentino	0–40	17	4,57E+24	26	74	0	NF 30% + SSrand 70%
19s	Tuscany–Emilia Apennines Shallow	0–15	12	6,50E+23	51	35	14	NF 50% + SS 35% + TFrاند 15%
19d	Tuscany–Emilia Apennines Deep	15,1–40	7	3,43E+24	3	3	93	TF 100%
20s	Emilia–Shallow	0–20	12	7,94E+23	0	2	98	TF 100%
20d	Emilia–Deep	20,1–40	3	6,20E+23	0	100	0	SS 100%
21	Ferrara–Arc	0–40	26	3,33E+25	0	2	98	TF 100%
22	Geothermal reg. Tuscany–Latium	0–40	0					
23	Trasimeno–Southern Latium	0–40	4	2,20E+23	0	100	0	SSrand 100%
24	Umbria–Abruzzo	0–40	104	2,22E+26	98	2	0	NF 100%
25s	Inner part of Marche	0–12,5	4	4,71E+24	14	86	0	SSrand 85% + NFrاند 15%
25d	Inner part of Marche	12,6–40	6	2,60E+23	0	77	23	SSrand 75% + TFrاند 25%
26	Rimini–Conero–Majella	0–40	14	2,21E+24	0	63	37	TF 40% + SSrand 60%

27	Northern Tyrrhenian Coast	0–40	4					
28	Colli Albani	0–40	0					
29	Chieti-Pescara	0–40	6	3,50E+23	0	17	83	TF-80% + SSrand-20%
30	Central-Adriatic Sea	0–40	22	7,46E+24	5	19	77	TF-80% + SS-20%
31	Ischia-Vesuvio	0–40	0					
32	Campania-part of the Tyrrhenian coast	0–40	3	2,53E+25	98	2	0	NFrاند-100%-
33	Sannio-Irpinia	0–40	23	2,62E+26	98	2	0	NF-100%
34	Gargano	0–40	15	1,12E+25	0	92	8	SS-100%
35	Ofanto	0–40	8	2,81E+25	50	50	0	NF-50%+SSrand-50%
36	Potenza-Matera	0–40	6	6,57E+24	1	99	0	SS-100%-
37	Southern-Puglia	0–40	0					
38	Otranto channel	0–40	1					
39	Calabrian-part of the Tyrrhenian coast	0–40	11	6,50E+26	100	0	0	NF-100%
40	Calabrian-part of the Ionian coast-	0–40	8	5,74E+24	15	83	2	NFrاند-15% + SSrand-85%
41	Ionian-Sea	0–40	13	5,60E+24	0	96	4	SS-100%-
42	Sardegna-Corsica	0–40	9	2,96E+24	0	1	99	TFrand-100%
43	Ustica-Alicudi	0–40	24	2,06E+25	0	56	44	TF-45%+SS-55%
44	Eolie-Patti	0–40	16	1,55E+25	2	97	1	SSrand-100%
45	Cefalù	0–40	12	2,44E+24	23	77	0	NF-25% + SSrand-75%
46	Western-Sicily	0–40	7	1,18E+25	0	97	3	SS-100%
47	Malta-Lampedusa	0–40	12	3,52E+24	1	79	20	SS-80% + TFrand-20%
48	Iblei	0–40	4	4,15E+23	0	87	13	SS-90% + TFrand-10%
49	Etna	0–40	8	4,60E+23	0	100	0	SS-100%
50	Southern Tyrrhenian-Sea	0–40	8	2,49E+24	53	30	17	NFrاند-50%+ SS-30%+ TFrand-20%

Kostrov, V. V.: Seismic moment and energy of earthquakes and seismic flow of rocks, Izv. Acad. Sci. USSR, Phys. Solid Earth, 1, 23–40, 1974.

Pagani, M., Monelli, D., Weatherill, G., Danciu, L., Crowley, H., Silva, V., et al.: OpenQuake engine: An open hazard (and risk) software for the global earthquake model. Seismological Research Letters, 85(3), 692–702. <https://doi.org/10.1785/0220130087>, 2014.

Pondrelli, S., Ekström, G. and Morelli, A.: Seismotectonic re-evaluation of the 1976 Friuli, Italy, seismic sequence, J. Seismology, 5(1), 73–83, <https://doi.org/10.1023/a:1009822018837>, 2001.

Pondrelli, S., Morelli, A., Ekström, G., Mazza, S., Boschi, E. and Dziewonski, A. M.: European-Mediterranean regional centroid-moment tensors: 1997-2000, Phys. Earth Planet. Int., 130, 71-101, 2002.

Pondrelli, S., Salimbeni, S., Ekström, G., Morelli, A., Gasperini, P. and Vannucci, G.: The Italian CMT dataset from 1977 to the present, Phys. Earth Planet. Int.,

doi:10.1016/j.pepi.2006.07.008,159/3-4, pp. 286-303, 200Table 2—Results of summation for each tectonic style (NF= normal; SS= strike-slip; TF= thrust) for all seismic zones in ZS16.

N.	-Seismic Zone-Name	NF-M ₀ (Dyn-cm)	NF events	NF strike, dip, rake	SS-M ₀ (Dyn-cm)	SS events	SS strike, dip, rake	TF-M ₀ (Dyn-cm)	TF events	TF strike, dip, rake
1	Idria				3,86E+24	7	219, 67, -2	9,00E+22	2	
2	Slovenia				1,18E+24	3	135, 68, 160	1,70E+23	3	131, 25, 66
3	Friuli				1,01E+25	13	293, 86, -178	8,14E+25	16	274, 25, 112
4	Valtellina-Alto-Adige				5,50E+23	2		1,46E+23	1	
5	Innsbruck				7,03E+23	1				
6	Grigioni	1,00E+24	4	295, 38, -77	1,12E+23	4				
7	Garda-Soncino	1,27E+23	1		6,50E+23	2		4,70E+23	3	234, 26, 90
8	Montreux		1							
9	Vallese				9,10E+23	7	102, 25, -107			
10	Western-Alps	3,40E+23	4	284, 37, -89	4,47E+24	9	310, 15, -32			
11	Piemonte	2,26E+23	1		1,73E+24	7	222, 74, -164	2,00E+22	2	
12	Mantova-Verona				7,80E+23	4	104, 60, -150	2,50E+23	2	
13	Pianura veneta									
14	Imperiese	3,27E+23	1		1,12E+23	1		1,48E+23	2	
15	Mar-Ligure				6,50E+23	3	264, 57, 169	1,35E+25	3	220, 45, 123
16	Tortona-Bobbio	1,50E+23	2		9,70E+23	7	110, 36, -135	5,00E+22	2	
17	Spezia-North of Tuscany	1,20E+23	2		3,10E+23	5	88, 67, -172	2,28E+22	1	
18	Lunigiana-Casentino	1,17E+24	11	308, 35, -90	3,40E+24	6	288, 35, -118			
19	Tuscany-Emilia Apennines Shallow	3,30E+23	7	309, 44, -99	2,30E+23	3	342, 39, -45	9,00E+22	2	
19	Tuscany-Emilia Apennines Deep	1,10E+23	1		1,20E+23	2		3,20E+24	4	278, 34, 84
20	Emilia Shallow				1,44E+22	1		7,80E+23	11	299, 36, 87
20	Emilia-Deep				6,20E+23	3	9, 38, 26			
21	Ferrara-Are				7,20E+23	9	40, 66, 16	3,26E+25	17	90, 33, 66
22	Geothermal reg. Tuscany Latium									
23	Trasimeno-Southern Latium				2,20E+23	4	228, 3, 64			
24	Umbria-Abruzzo	2,18E+26	89	321, 37, -86	3,47E+24	15	164, 31, -65			
25	Inner-part-of Marche	6,60E+23	2		4,05E+24	2				
25	Inner-part-of Marche				2,00E+23	5	104, 76, -176	6,00E+22	1	
26	Rimini-Genere-Majella				1,40E+24	9	117, 49, 15	8,10E+23	5	112, 38, 61

27	Northern Tyrrhenian Coast					4				
28	Colli Albani									
29	Chieti-Pescara				6,00E+22	2		2,90E+23	4	191, 44, 64
30	Central Adriatic-Sea	3,44E+23	1		1,39E+24	3	267, 71, -9	5,73E+24	18	286, 44, 92
31	Ischia-Vesuvio									
32	Campania part-of-the Tyrrhenian coast	2,48E+25	4		5,20E+23	2				
33	Sannio-Irpinia	2,57E+26	20	135, 40, -80	5,12E+24	3	190, 42, -39			
34	Gargano				1,03E+25	11	176, 73, 0	8,80E+23	4	205, 33, 66
35	Ofanto	1,41E+25	3	168, 31, -55	1,40E+25	5	163, 67, 171			
36	Potenza-Matera	8,47E+22	1		6,49E+24	5	184, 73, -10			
37	Southern Puglia									
38	Otranto channel				6,00E+23	1				
39	Calabrian part-of-the Tyrrhenian coast	6,49E+26	7	358, 39, -113	4,10E+23	4	331, 61, 171			
40	Calabrian part-of-the Ionian coast	8,36E+23	1		4,76E+24	5	300, 64, -165	1,40E+23	2	
41	Ionian-Sea				5,37E+24	11	278, 59, 171	2,30E+23	2	
42	Sardegna-Gorsica				2,94E+22	1		2,93E+24	8	237, 34, 87
43	Ustica-Alicudi				1,16E+25	3	24, 45, 41	9,03E+24	21	72, 38, 90
44	Eolie-Patti	2,70E+23	4	16, 32, -105	1,50E+25	9	135, 60, -176	2,20E+23	3	294, 32, 96
45	Cefalù	5,70E+23	5	100, 36, -111	1,87E+24	7	21, 14, -148			
46	Western Sicily				1,15E+25	6	268, 50, 33	3,09E+23	1	
47	Malta-Lampedusa	2,51E+22	1		2,79E+24	9	189, 70, -5	7,00E+23	2	
48	Iblei				3,60E+23	3	190, 80, 4	5,54E+22	1	
49	Etna				4,60E+23	8	46, 68, 20			
50	Southern Tyrrhenian Sea	1,31E+24	3	18, 35, -111	7,50E+23	4	253, 11, -29	4,33E+23	1	

Pondrelli, S. and Salimbeni, S.: Regional Moment Tensor Review: An Example from the European Mediterranean Region. In Encyclopedia of Earthquake Engineering (pp. 1-15). http://link.springer.com/referenceworkentry/10.1007/978-3-642-36197-5_301-1, Springer Berlin Heidelberg, 2015.

Roselli, P., Marzocchi, W., Mariucci M. T. and Montone, P.: Earthquake focal mechanism forecasting in Italy for PSHA purposes. Geophys. J. Int., 212, 491–508, doi: [10.1093/gji/ggx383](https://doi.org/10.1093/gji/ggx383), 2017.

Rovida, A., Locati, M., Camassi, R., Lolli, B., Gasperini, P. (eds): CPT15, the 2015 version of the Parametric Catalogue of Italian Earthquakes. Istituto Nazionale di Geofisica e Vulcanologia. doi:<http://doi.org/10.6092/INGV.IT-CPT15>, 2016, last access: 15 July 2020.

Saul, J., Becker, J., Hanka, W.: Global moment tensor computation at GFZ Potsdam, AGU 2011 Fall Meeting, 2011.

Serpelloni, E., M. Anzidei, P. Baldi, G. Casula, A. Galvani: Crustal velocity and strain-rate fields in Italy and surrounding regions: new results from the analysis of permanent and non-permanent GPS networks, Geophysical Journal International, 161, 3, 861–880, <https://doi.org/10.1111/j.1365-246X.2005.02618.x>, 2005.

Stucchi, M., Meletti, C., Montaldo, V., Crowley, H., Calvi, G.M., and Boschi, E.: Seismic Hazard Assessment (2003–2009) for the Italian Building Code, Bull. Seismol. Soc. Am. 101, 4, 1885–1911, 2011.

Vannucci, G. and Gasperini, P.: The new release of the database of Earthquake Mechanisms of the Mediterranean Area (EMMA Version 2), Annals of Geophysics, Suppl. V, 47, N.1, 307-334, 2004.

Wessel, P., & Smith, W. H. F. (1998). New, improved version of Generic Mapping Tools released. Eos, Transactions American Geophysical Union, 79(47), 579. <https://doi.org/10.1029/98EO00426>

Table 3 — List of recent earthquakes compared to the results of this study.

ID event	Date (yyyy-mm-dd)	Time-UTC	Lat	Long	Depth (km)	Mw
1	2016-02-08	15:35:43.39	36.97	14.86	-7.4	4.2
2	2016-08-24	01:36:32.00	42.69	13.23	-8.1	6.0
3	2016-10-30	06:40:17.32	42.83	13.10	10.0	6.5
4	2017-01-18	10:14:09.90	42.53	13.28	-9.6	5.5
5	2017-02-03	04:10:05.32	42.99	13.01	-7.1	4.2
6	2017-11-19	12:37:44.70	44.66	10.03	22.4	4.4
7	2018-04-10	03:11:30.76	43.06	13.03	-8.1	4.6
8	2018-08-14	21:48:30.98	41.88	14.84	19.2	4.6
9	2018-08-16	18:19:04.60	41.87	14.86	19.6	5.1
10	2018-10-06	00:34:19.79	37.60	14.93	-4.5	4.6
11	2018-12-26	02:19:14.00	37.64	15.11	-10.0	4.9
12	2019-01-14	23:03:57.02	44.34	12.28	20.6	4.3

TABLES

Table 1 - Data for each seismic zone, including seismogenic thickness used for the summation of focal mechanisms, number of available focal mechanisms, cumulative M_{0sum} and cumulative focal mechanism for each tectonic style (NF, SS, TF). "s" and "d" added to the seismic zone number refer to shallow and deep zones, when the summation is done for different depth intervals.

N.	Seismic Zone	Thic kne ss (km)	n. N E	NF M_{0sum} (dyn cm)	cumulative NF strike, dip, rake	n. SS	SS M_{0sum} (dyn cm)	cumulative SS strike, dip, rake	n. T F	TF M_{0sum} (dyn cm)	cumulative TF strike, dip, rake
1	Idria	0-40	==	==	==	7	3.86E+2 4	219, 67, -2	2	9.00E+2 2	==
2	Slovenia	0-40	==	==	==	3	1.18E+2 4	135, 68, 160	3	1.70E+2 3	131, 25, 66
3	Friuli	0-40	==	==	==	13	1.01E+2 5	293, 86, -178	1 6	8.14E+2 5	274, 25, 112
4	Valtellina - Alto Adige	0-40	==	==	==	2	5.50E+2 3	==	1	1.46E+2 3	==
5	Innsbruck	0-40	==	==	==	1	7.03E+2 3	==	==	==	==
6	Grigioni	0-40	4	1.00E+2 4	295, 38, -77	1	1.12E+2 3	==	==	==	==
7	Garda- Soncino	0-40	1	1.27E+2 3	==	2	6.50E+2 3	==	3	4.70E+2 3	234, 26, 90
8	Montreux	0-40	1	==	==	==	==	==	==	==	==
9	Vallese	0-40	==	==	==	7	9.10E+2 3	102, 25, -107	==	==	==
10	Western Alps	0-40	4	3.40E+2 3	284, 37, -89	9	4.47E+2 4	310, 15, -32	==	==	==
11	Piemonte	0-40	1	2.26E+2 3	==	7	1.73E+2 4	222, 74, -164	2	2.00E+2 2	==
12	Mantova Verona	0-40	==	==	==	4	7.80E+2 3	104, 60, -150	2	2.50E+2 3	==
13	Pianura veneta	0-40	==	==	==	==	==	==	==	==	==
14	Imperiese	0-40	1	3.27E+2 3	==	1	1.12E+2 3	==	2	1.48E+2 3	==
15	Mar Ligure	0-40	==	==	==	3	6.50E+2 3	264, 57, 169	3	1.35E+2 5	220, 45, 123
16	Tortona- Bobbio	0-40	2	1.50E+2 3	==	7	9.70E+2 3	110, 36, -135	2	5.00E+2 2	==
17	Spezia North of Tuscany	0-40	2	1.20E+2 3	==	5	3.10E+2 3	88, 67, -172	1	2.28E+2 2	==
18	Lunigiana- Casentino	0-40	1 1	1.17E+2 4	308, 35, -90	6	3.40E+2 4	288, 35, -118	==	==	==
19 s	Tuscany- Emilia Apennines Shallow	0-15	7	3.30E+2 3	309, 44, -99	3	2.30E+2 3	342, 39, -45	2	9.00E+2 2	==
19 d	Tuscany- Emilia Apennines Deep	15.1 -40	1	1.10E+2 3	==	2	1.20E+2 3	==	4	3.20E+2 4	278, 34, 84
20 s	Emilia Shallow	0-20	==	==	==	1	1.44E+2 2	==	1 1	7.80E+2 3	299, 36, 87
20 d	Emilia Deep	20.1 -40	==	==	==	3	6.20E+2 3	9, 38, 26	==	==	==
21	Ferrara Arc	0-40	==	==	==	9	7.2E+23	40, 66, 16	1 7	3.26E+2 5	90, 33, 66

22	Geothermal reg. Tuscany Latium	0-40	=	=	=	=	=	=	=	=	=
23	Trasimeno-Southern Latium	0-40	=	=	=	4	2.2E+23	228, 3, 64	=	=	=
24	Umbria-Abruzzo	0-40	8 9	2.18E+2 6	321, 37, -86	15	3.47E24	164, 31, -65	=	=	=
25	Inner part of Marche	0-12.5	2	6.60E+2 3		2	4.05E24		=	=	=
25	Inner part of Marche	12.6-40	=	=	=	5	2.00E23	104, 76, -176	1	6.00E+2 2	=
26	Rimini-Conero-Majella	0-40	=	=	=	9	1.40E+2 4	117, 49, 15	5	8.10E+2 3	112, 38, 61
27	Northern Tyrrhenian Coast	0-40	=	=	=	1	1.77E23	=	=	=	=
28	Colli Albani	0-40	=	=	=	=	=	=	=	=	=
29	Chieti-Pescara	0-40	=	=	=	2	6.00E22	=	4	2.90E+2 3	191, 44, 64
30	Central Adriatic Sea	0-40	1	3.44E+2 3	=	3	1.39E+2 4	267, 71, -9	1 8	5.73E+2 4	286, 44, 92
31	Ischia-Vesuvio	0-40	=	=	=	=	=	=	=	=	=
32	Campania part of the Tyrrhenian coast	0-40	1	2.48E+2 5	=	2	5.20E+2 3	=	=	=	=
33	Sannio-Irpinia	0-40	2 0	2.57E+2 6	135, 40, -80	3	5.12E+2 4	190, 42, -39	=	=	=
34	Gargano	0-40	=	=	=	11	1.03E+2 5	176, 73, 0	4	8.80E+2 3	205, 33, 66
35	Ofanto	0-40	3	1.41E+2 5	168, 31, -55	5	1.40E+2 5	163, 67, 171	=	=	=
36	Potenza-Matera	0-40	1	8.47E+2 2	=	5	6.49E+2 4	184, 73, 10	=	=	=
37	Southern Puglia	0-40	=	=	=	=	=	=	=	=	=
38	Otranto channel	0-40	=	=	=	1	6.00E+2 3	=	=	=	=
39	Calabrian part of the Tyrrhenian coast	0-40	7	6.49E+2 6	358, 39, -113	4	4.10E+2 3	331, 61, 171	=	=	=
40	Calabrian part of the Ionian coast	0-40	1	8.36E+2 3	=	5	4.76E+2 4	300, 64, -165	2	1.40E+2 3	=
41	Ionian Sea	0-40	=	=	=	11	5.37E+2 4	278, 59, 171	2	2.30E+2 3	=
42	Sardegna-Corsica	0-40	=	=	=	1	2.94E+2 2		8	2.93E+2 4	237, 34, 87
43	Ustica-Alicudi	0-40	=	=	=	3	1.16E+2 5	24, 45, 41	2 1	9.03E+2 4	72, 38, 90
44	Eolie-Patti	0-40	4	2.70E+2 3	16, 32, -105	9	1.50E+2 5	135, 60, -176	3	2.20E+2 3	294, 32, 96
45	Cefalù	0-40	5	5.70E+2 3	100, 36, -111	7	1.87E+2 4	21, 14, -148	=	=	=
46	Western Sicily	0-40	=	=	=	6	1.15E+2 5	268, 50, 33	1	3.09E+2 3	=
47	Malta Lampedusa	0-40	1	2.51E+2 2	=	9	2.79E+2 4	189, 70, -5	2	7.00E+2 3	=

48	Iblei	0-40	=	=	=	3	3.60E+2 3	190, 80, 4	1	5.54E+2 2	=
49	Etna	0-40	=	=	=	8	4.60E+2 3	46, 68, 20			=
50	Southern Tyrrhenian Sea	0-40	3	1.31E+2 4	18, 35, -111	4	s	253, 11, -29	1	4.33E+2 3	=

Table 2 - Results of the evaluation of P-, T- and B- axis dispersion. In each column is reported Δ , in degrees, i.e. the median of the angular differences between the axes of each single focal mechanism and the axes of the cumulative one (see Figure 4).

38	Otranto channel	=	=	=	0	1	=	0	1	=
39	Calabrian part of Tyrrhenian coast	3	25	3	26	34	22	26	34	22
40	Calabrian part of Ionian coast	=	=	=	74	22	56	74	22	56
41	Ionian Sea	=	=	=	36	30	3	36	30	3
42	Sardegna-Corsica	=	=	=	=	=	=	16	48	47
43	Ustica-Alicudi	=	=	=	57	18	20	14	16	16
44	Eolie-Patti	8	6	8	56	48	39	2	25	30
45	Cefalù	16	17	22	27	48	4	27	48	4
46	Western Sicily	=	=	=	17	13	12	17	13	12
47	Malta-Lampedusa	=	=	=	25	20	32	25	20	32
48	Iblei	=	=	=	24	19	11	24	19	11
49	Etna	=	=	=	40	28	5	40	28	5
50	Southern Tyrrhenian Sea	49	45	17	24	22	20	24	22	20

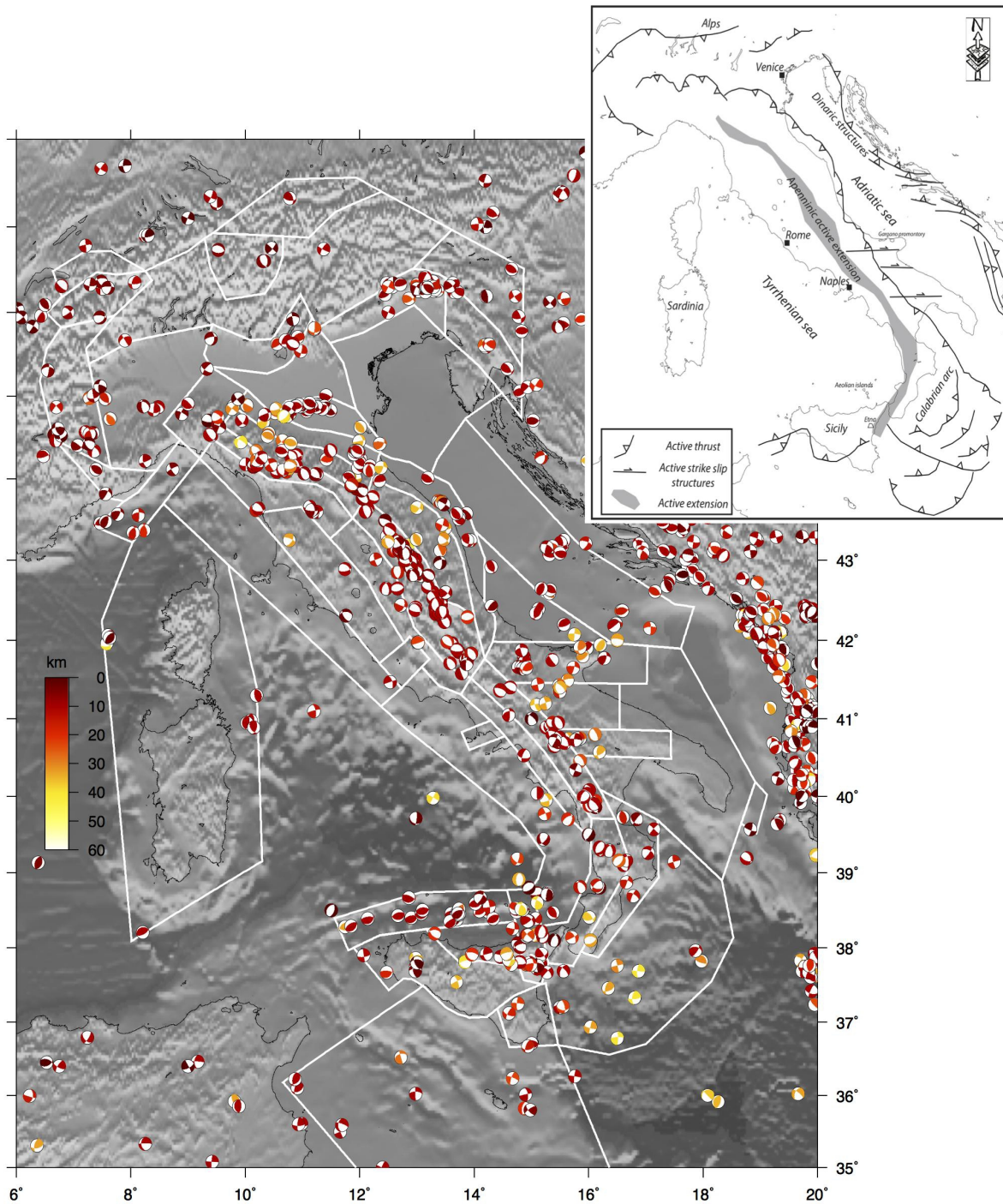


Figure 1— Map of the entire dataset used for this study (see data in Table 1_SupplementaryMaterial). Different colors for the focal mechanisms represent different hypocentral depths, following the scale on the left. In the background, the borders of the seismic source zones in ZS16 are reported in white. Top right, a seismotectonic sketch of the study region.

Table 3 - Final style-of-faulting for each seismic zone, with the total amount of used focal mechanisms, the total released seismic moment M_{0Total} per zone and the percentage of contribution of each tectonic style to the final source.

<u>N.</u>	<u>Seismic Zone Name</u>	<u>n. of focal mec.</u>	<u>M_{0Total} (dyn cm)</u>	<u>%NF</u>	<u>%SS</u>	<u>%TF</u>	<u>Final Style-of-faulting</u>
-----------	--------------------------	-------------------------	------------------------------------	------------	------------	------------	--------------------------------

1	<u>Idria</u>	9	<u>3.94E+2</u> 4	0	98	2	<u>SS100%</u>
2	<u>Slovenia</u>	6	<u>1.35E+2</u> 4	0	87	13	<u>SS85% + TF15%</u>
3	<u>Friuli</u>	29	<u>9.15E+2</u> 5	0	11	89	<u>TF90% + SS10%</u>
4	<u>Valtellina - Alto Adige</u>	3	<u>6.96E+2</u> 3	0	79	21	<u>SSrand80% + TFrاند20%</u>
5	<u>Innsbruck</u>	1	=	=	=	=	<u>random 100%</u>
6	<u>Grigioni</u>	5	<u>1.11E+2</u> 4	90	10	0	<u>NF100%</u>
7	<u>Garda-Soncino</u>	6	<u>1.25E+2</u> 4	10	52	38	<u>SSrand60%+TFrand40%</u> <u>(100%rand)</u>
8	<u>Montreux</u>	1	=	=	=	=	<u>random 100%</u>
9	<u>Vallese</u>	7	<u>9.10E+2</u> 3	0	100	0	<u>SSrand100%</u>
10	<u>Western Alps</u>	13	<u>4.81E+2</u> 4	7	93	0	<u>SSrand100%</u>
11	<u>Piemonte</u>	10	<u>1.98E+2</u> 4	11	88	1	<u>NFrاند10% + SSrand90%</u>
12	<u>Mantova-Verona</u>	6	<u>1.03E+2</u> 4	0	76	24	<u>SS75% + TFrاند25%</u>
13	<u>Pianura veneta</u>	0	=	=	=	=	<u>random 100%</u>
14	<u>Imperiese</u>	4	<u>5.87E+2</u> 3	56	19	25	<u>random100%</u>
15	<u>Mar Ligure</u>	6	<u>1.42E+2</u> 5	0	5	95	<u>TF100%</u>
16	<u>Tortona-Bobbio</u>	11	<u>1.17E+2</u> 4	13	83	4	<u>NFrاند15% + SSrand85%</u>
17	<u>Spezia-North of Tuscany</u>	8	<u>4.53E+2</u> 3	27	68	5	<u>SS70% + NFrاند30%</u>
18	<u>Lunigiana-Casentino</u>	17	<u>4.57E+2</u> 4	26	74	0	<u>NF30% + SSrand70%</u>
19s	<u>Tuscany-Emilia Apennines Shallow</u>	12	<u>6.50E+2</u> 3	51	35	14	<u>NF50% + SS35% + TFrاند15%</u>
19d	<u>Tuscany-Emilia Apennines Deep</u>	7	<u>3.43E+2</u> 4	3	3	93	<u>TF100%</u>
20s	<u>Emilia Shallow</u>	12	<u>7.94E+2</u> 3	0	2	98	<u>TF100%</u>
20d	<u>Emilia Deep</u>	3	<u>6.20E+2</u> 3	0	100	0	<u>SS100%</u>
21	<u>Ferrara Arc</u>	26	<u>3.33E+2</u> 5	0	2	98	<u>TF100%</u>
22	<u>Geothermal reg. Tuscany Latium</u>	0	=	=	=	=	<u>random 100%</u>
23	<u>Trasimeno Southern Latium</u>	4	<u>2.20E+2</u> 3	0	100	0	<u>SSrand100%</u>
24	<u>Umbria-Abruzzo</u>	104	<u>2.22E+2</u> 6	98	2	0	<u>NF100%</u>
25s	<u>Inner part of Marche</u>	4	<u>4.71E+2</u> 4	14	86	0	<u>SSrand85% + NFrاند15%</u>
25d	<u>Inner part of Marche</u>	6	<u>2.60E+2</u> 3	0	77	23	<u>SSrand75% + TFrاند25%</u>

26	Rimini-Conero Majella	14	2.21E+2 4	0	63	37	TF40% + SSrand 60%
27	Northern Tyrrhenian Coast	1	=	=	=	=	random 100%
28	Colli Albani	0	=	=	=	=	random 100%
29	Chieti-Pescara	6	3.50E+2 3	0	17	83	TF80% + SSrand20%
30	Central Adriatic Sea	22	7.46E+2 4	5	19	77	TF80% + SS20%
31	Ischia-Vesuvio	0	=	=	=	=	random 100%
32	Campania part of Tyrrhenian coast	3	2.53E+2 5	98	2	0	NFrاند100%
33	Sannio-Irpinia	23	2.62E+2 6	98	2	0	NF100%
34	Gargano	15	1.12E+2 5	0	92	8	SS100%
35	Ofanto	8	2.81E+2 5	50	50	0	NF50%+SSrand50%
36	Potenza-Matera	6	6.57E+2 4	1	99	0	SS100%
37	Southern Puglia	0	=	=	=	=	random 100%
38	Otranto channel	1	=	=	=	=	random 100%
39	Calabrian part of Tyrrhenian coast	11	6.50E+2 6	100	0	0	NF100%
40	Calabrian part of Ionian coast	8	5.74E+2 4	15	83	2	NFrاند15% + SSrand85%
41	Ionian Sea	13	5.60E+2 4	0	96	4	SS100%
42	Sardegna- Corsica	9	2.96E+2 4	0	1	99	TF ran 100%
43	Ustica-Alicudi	24	2.06E+2 5	0	56	44	TF45%+SS55%
44	Eolie-Patti	16	1.55E+2 5	2	97	1	SSrand100%
45	Cefalù	12	2.44E+2 4	23	77	0	NF25% + SSrand75%
46	Western Sicily	7	1.18E+2 5	0	97	3	SS100%
47	Malta- Lampedusa	12	3.52E+2 4	1	79	20	SS80% + TFrاند20%
48	Iblei	4	4.15E+2 3	0	87	13	SS90% + TFrاند10%
49	Etna	8	4.60E+2 3	0	100	0	SS100%
50	Southern Tyrrhenian Sea	8	2.49E+2 4	53	30	17	NFrاند50%+ SS30% + TFrand20%

Table 4 — List of earthquakes occurred after 2015, used in the comparison with the results of this study.

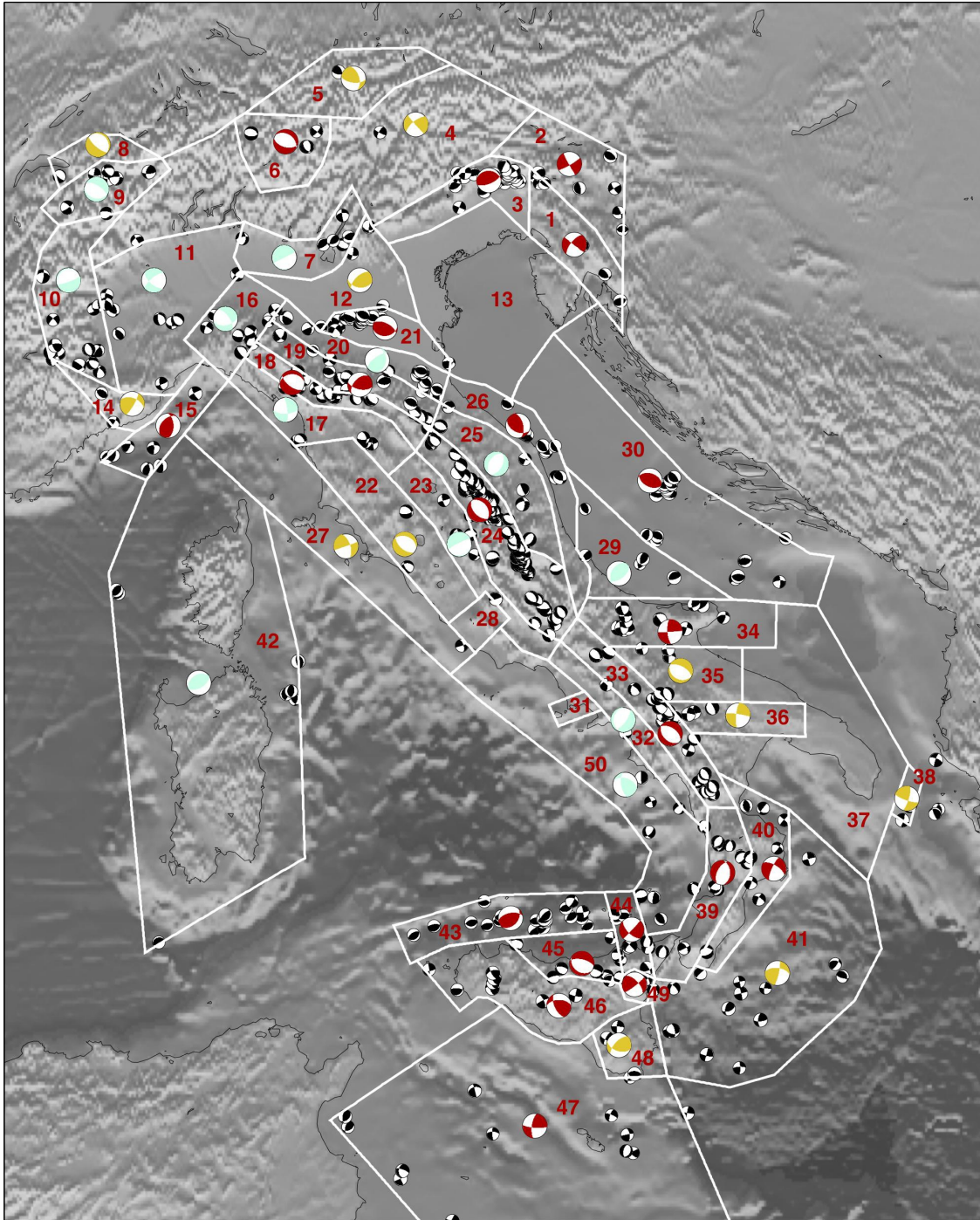


Figure 2— Results of summation using a 20-km seismogenic layer thickness for all the seismic zones. Coloured focal mechanisms are the result of the summations: red ones represent stable cumulative focal mechanisms, yellow are less reliable (low number of events to cumulate), light blue are unstable because of the heterogeneity of the input dataset. In the background: the entire available dataset in black; in white the seismic zones in ZS16 numbered in red.

ID event	Date (yyyy-mm-dd)	Time UTC	Lat	Long	Depth (km)	Mw
1	2016-02-08	15:35:43.39	36.97	14.86	7.4	4.2
2	2016-08-24	01:36:32.00	42.69	13.23	8.1	6.0

3	2016-10-30	06:40:17.32	42.83	13.10	10.0	6.5
4	2017-01-18	10:14:09.90	42.53	13.28	9.6	5.5
5	2017-02-03	04:10:05.32	42.99	13.01	7.1	4.2
6	2017-11-19	12:37:44.70	44.66	10.03	22.4	4.4
7	2018-04-10	03:11:30.76	43.06	13.03	8.1	4.6
8	2018-08-14	21:48:30.98	41.88	14.84	19.2	4.6
9	2018-08-16	18:19:04.60	41.87	14.86	19.6	5.1
10	2018-10-06	00:34:19.79	37.60	14.93	4.5	4.6
11	2018-12-26	02:19:14.00	37.64	15.11	10.0	4.9
12	2019-01-14	23:03:57.02	44.34	12.28	20.6	4.3

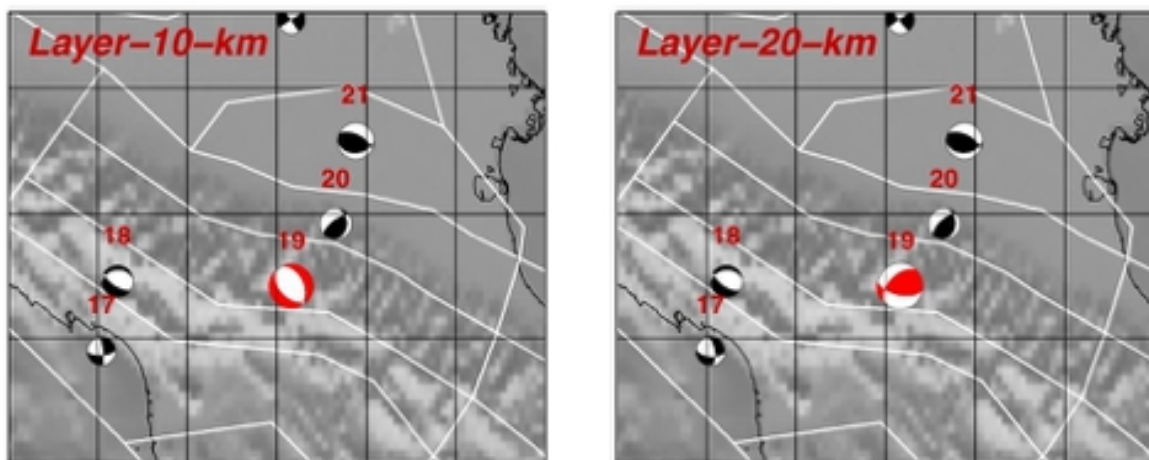


Figure 3—Example of tectonic style layering, for the seismic zone n. 19. The cumulative moment tensor for 10 km of seismogenic layer thickness shows a completely different result with respect to the one given by 20 km of thickness. Red numbers indicate the seismic zones.

FIGURES and CAPTIONS

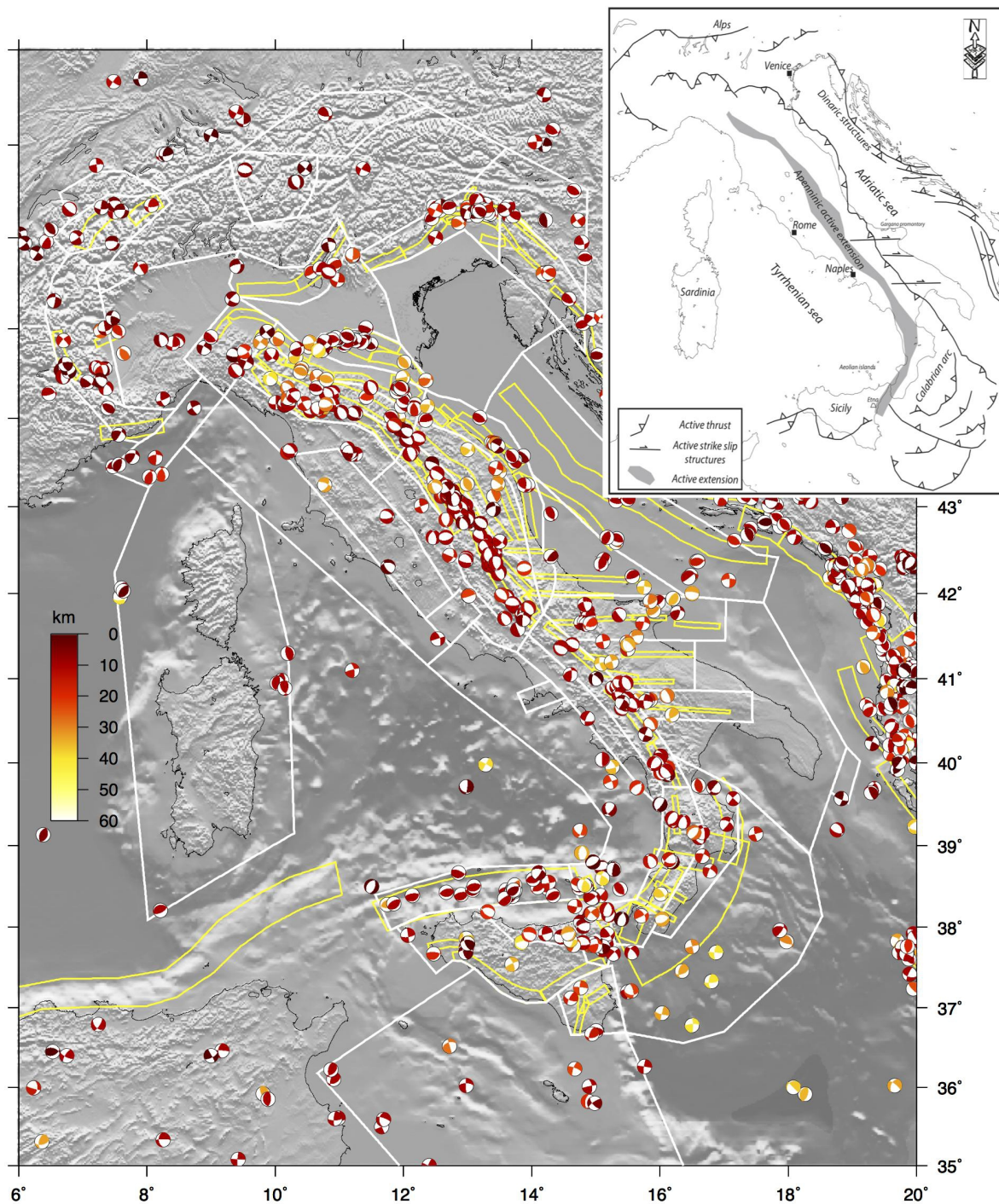
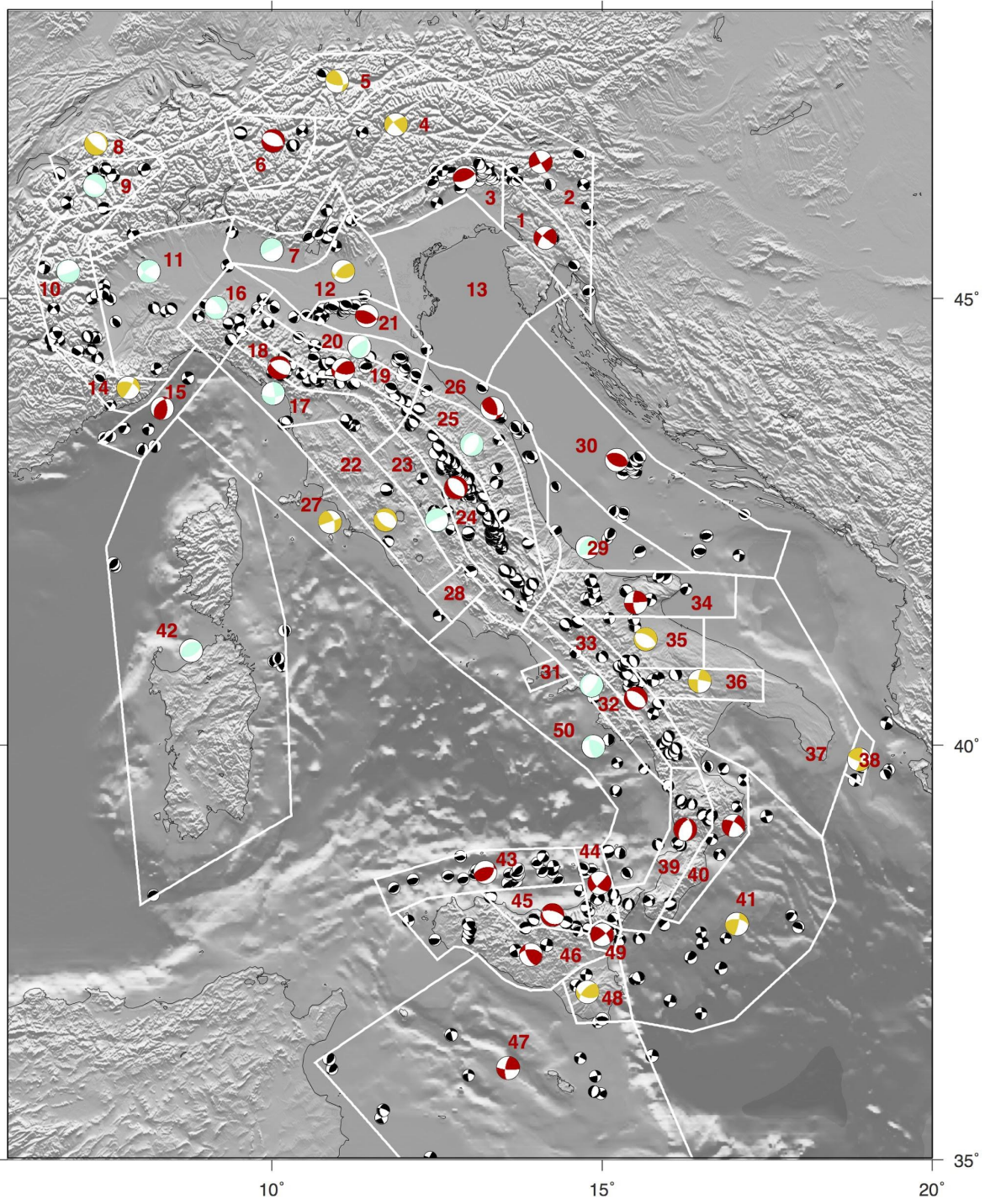


Figure 1 - Map of the entire available dataset. Different colors of the focal mechanisms represent different hypocentral depths, following the scale on the left. On the background, the borders of the seismic source zones of ZS16 (Meletti et al., 2019) are reported in white; in yellow, Composite Seismogenic Sources taken from DISS database (DISS Working Group, 2018; <http://diss.rm.ingv.it/diss>). Top right, map of main tectonic features of the study region. Example of data dispersion analysis for the seismic zone n.9. On the left is drawn the possible cumulative focal mechanism obtained with the summation of all input data, all strike slip. On the right, the dispersion plots where P, T and B axes of the cumulative and the single input data are compared. The angular difference between P and T axes is greater than 30° , and the final solution is a strike slip, but random (see Table 1).



E

Figure 2 - Map of the results of a test of focal mechanisms summation for each seismic zone in ZS16 (contoured in white, numbered in red) using a 20 km seismogenic layer thickness. Obtained cumulative focal mechanisms are in red when considered a stable result, yellow when less reliable, light blue when too uncertain because of the heterogeneity of input data (see in the text for quality evaluation criteria). On the background, the small black focal mechanisms are the input dataset.

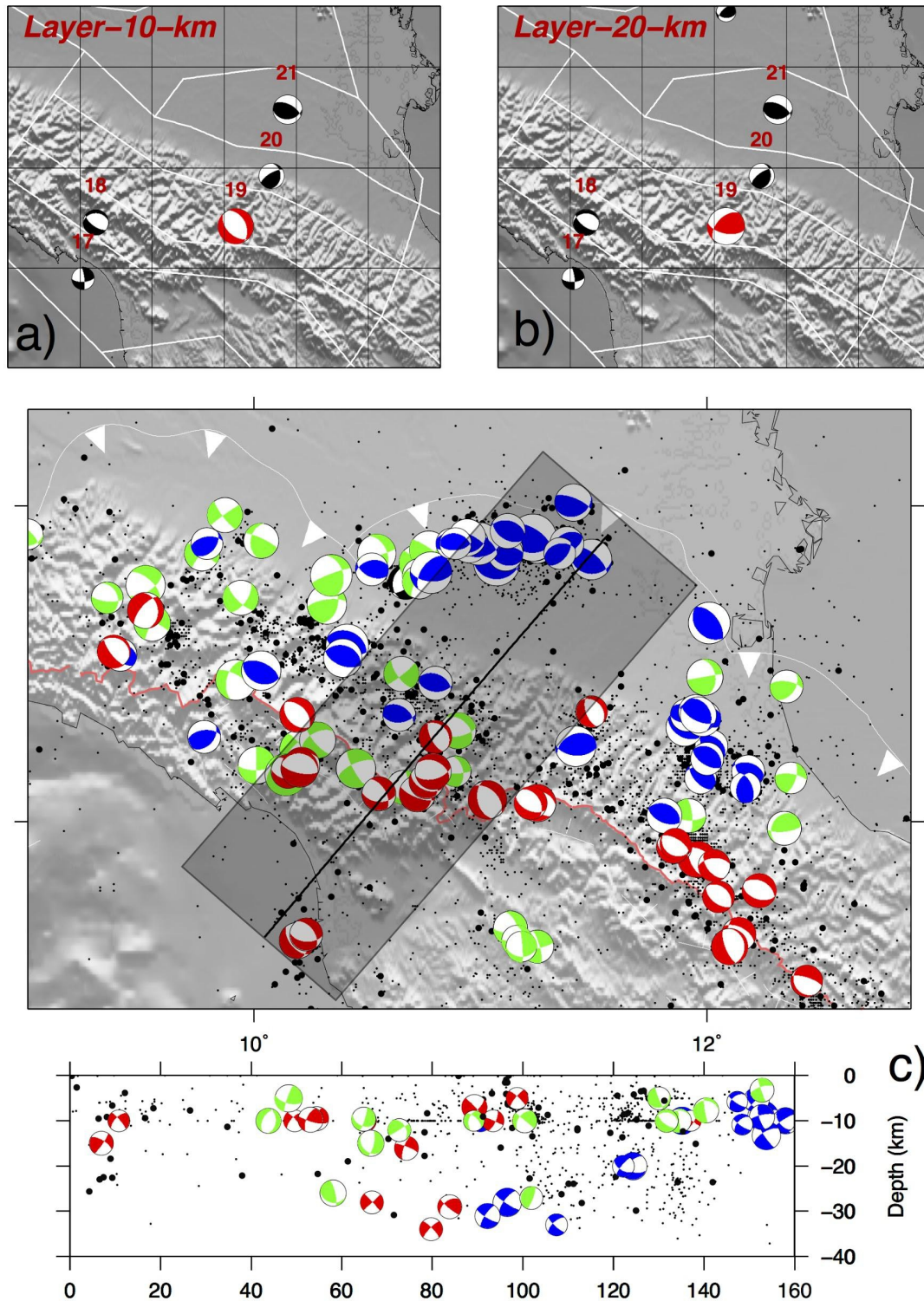


Figure 3 - a) and b) are an example of tectonic style layering, for the seismic zone n. 19. The cumulative moment tensor obtained for 10 km of thickness shows a completely different result with respect to the one given by 20 km. Red numbers indicate the seismic zones. c) map and section of our dataset in the region of the seismic zone n.19; red, green and blue focal mechanisms are respectively normal, strike-slip and reverse type. Seismicity in the background (black dots, smaller are for events with $M < 3$) is from ISIDE Working Group. (2007)

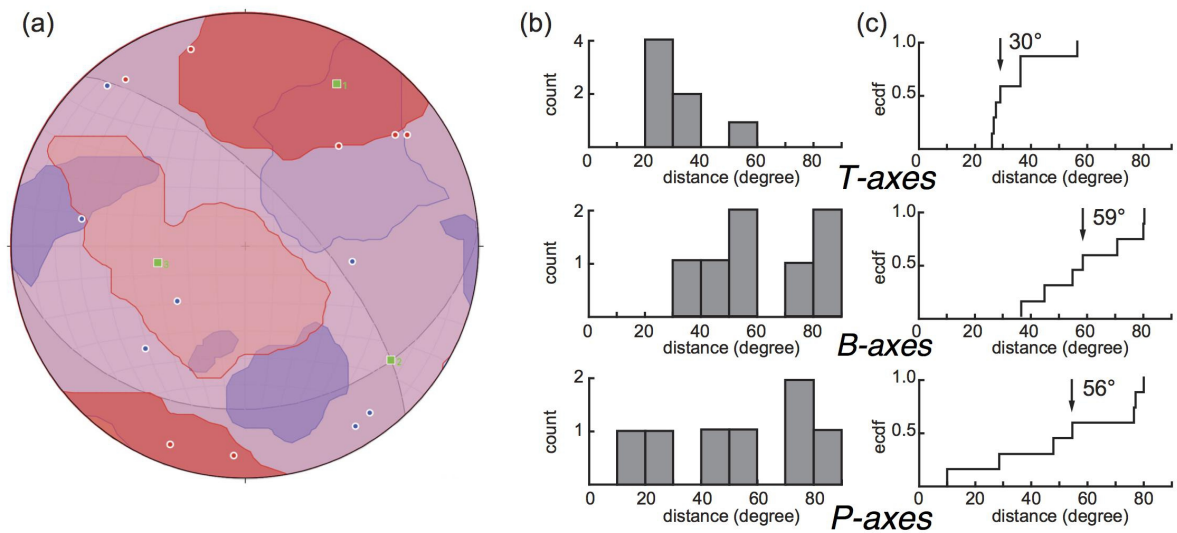


Figure 4 - An example of dispersion analysis for data of the seismic zone n.9. a) the possible cumulative focal mechanism obtained with the summation of all focal mechanisms available for this zone, all strike slip. Blue and red circles are P- and T- axes of input focal mechanisms, green symbols are P-, T- and B- axes of the cumulative one; blue and red areas are P- and T- axes contours. b) histograms and c) cumulative curve of the angular difference between T- (top), B- (middle) and P- (bottom) axes of input and cumulative focal mechanisms. c) cumulative plots. Black arrows: median value. 5—Map of the expected tectonic style obtained for each seismic zone. Circles represent random seismic sources: white circles are tectonically random sources, blue circles are thrust random sources, red and green circles are normal random and strike-slip random sources, respectively. Same colours refer also to cumulative focal mechanisms that have dimensions proportional to their percentage of contribution with respect to the total cumulative M_0 . Focal mechanisms with the grey background or circles with a grey border represent the cumulative source for deeper layers. When more than a symbol is reported in a zone, the final seismic source defined there includes several components, i.e. 90% of the seismic source is normal and 10% is strike-slip random.

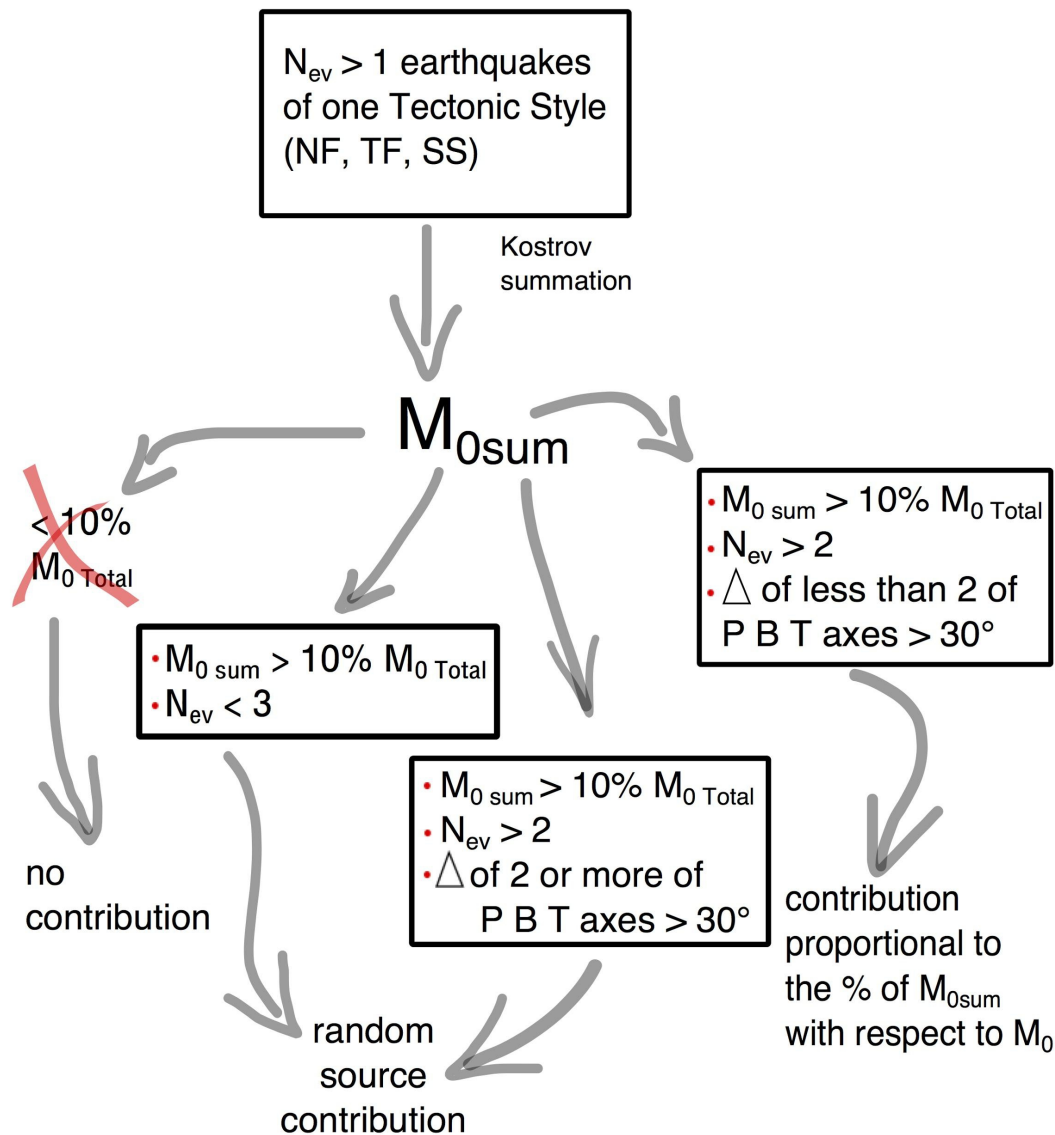


Figure 5 - Sketch of the decision making process applied to each zone and to each tectonic style group of earthquakes. N_{ev} is the number of available earthquakes; M_{0sum} is the seismic moment obtained summing the $N_{ev} \cdot M_0$; M_{0Total} is the cumulative seismic moment release in the singular zone independently from the tectonic style of events; Δ is the angular distance between P-, T- and B- axes of single focal mechanism involved in the summation and those of the cumulative one.

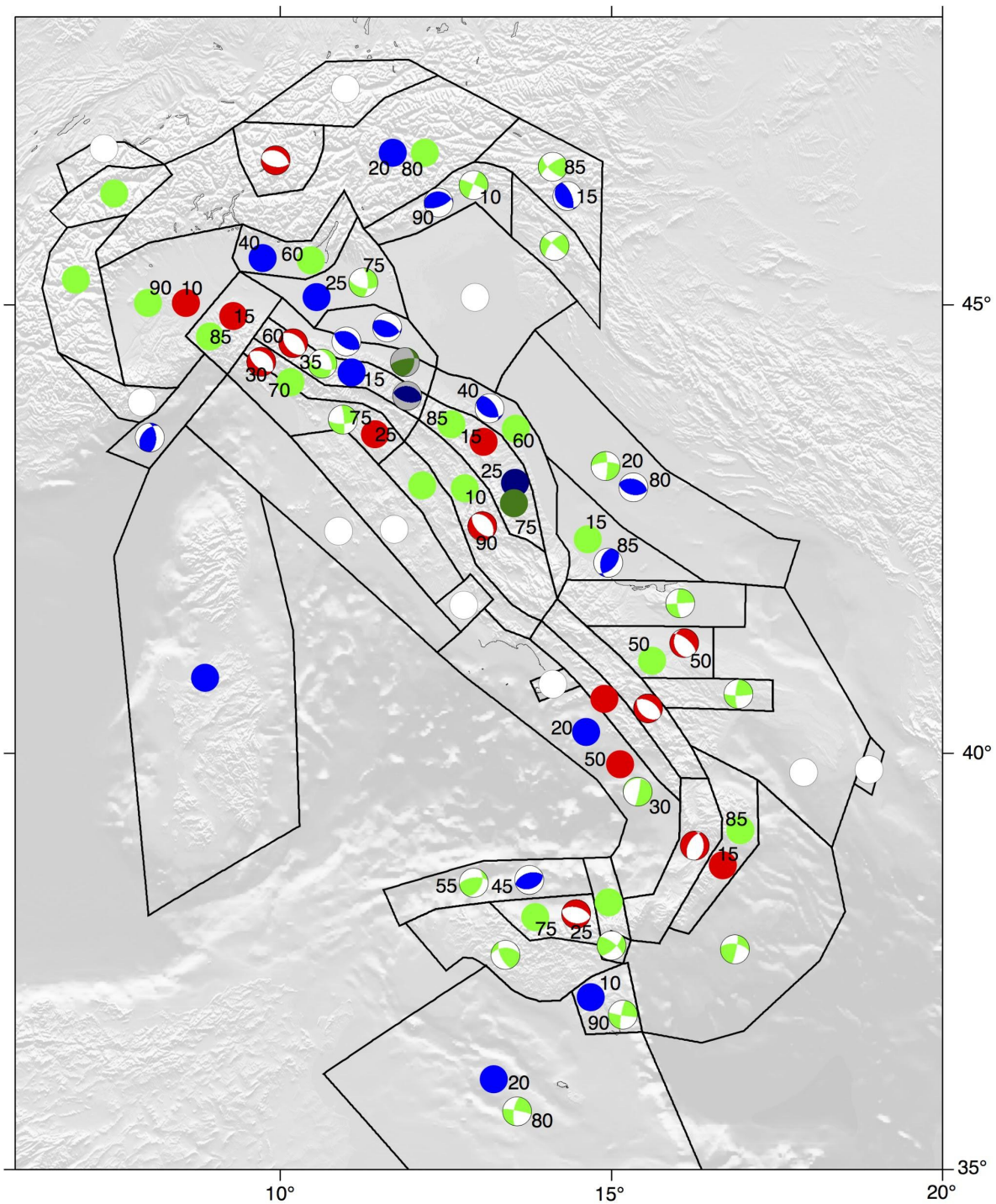


Figure 6 - Map of the expected style-of-faulting obtained for each seismic zone. Full circles represent random seismic sources: white circles are 100% random; blue, red and green circles are reverse, normal and strike-slip random sources, respectively. Same colors refer also to cumulative focal mechanisms. Focal mechanisms with a grey background or circles with darker colors represent the sources for deeper layers. Numbers in black are the percentage of contribution to the final source when it is composed by different styles— Comparison of recent earthquakes seismic moment tensors (in black, Table 3) and the expected tectonic style we identified in the same seismic zone (for colors see Figure 5). Focal mechanisms with a grey background belong to deeper sources. White numbers indicate the seismic zones, while black numbers refer to seismic events listed in Table 3.

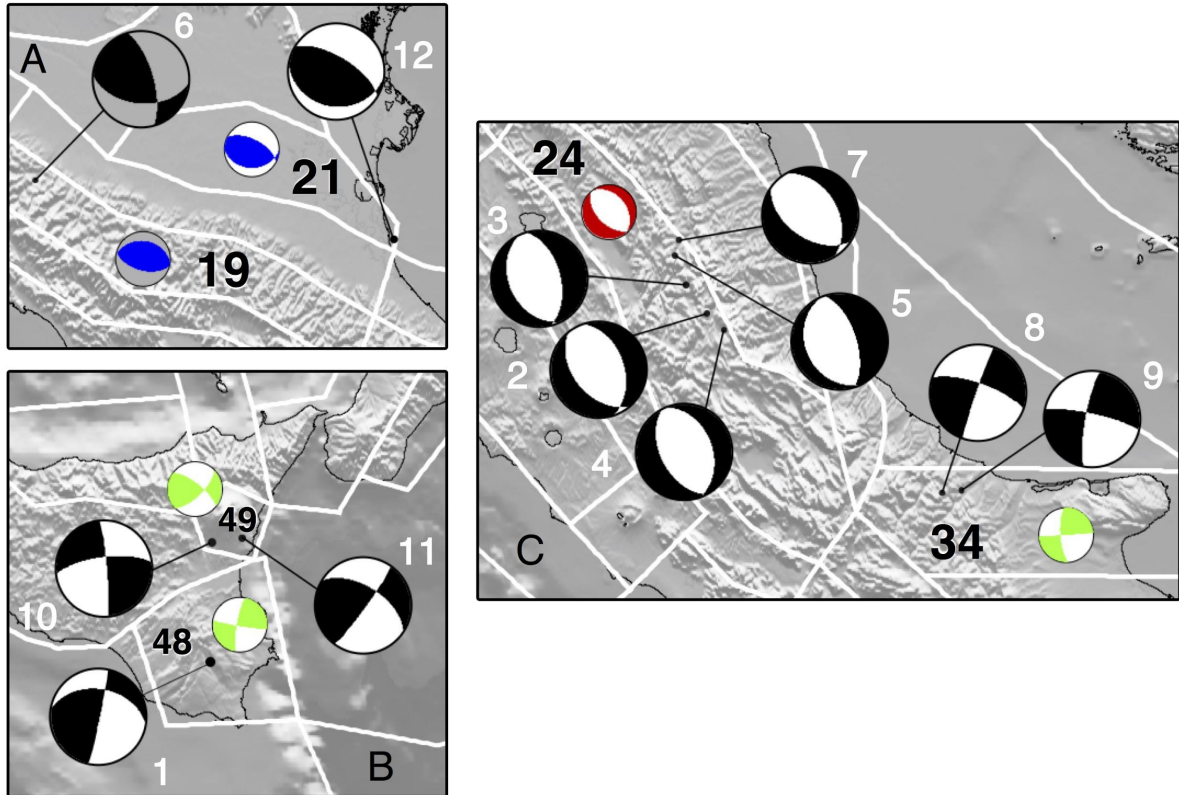


Figure 7 — Comparison of seismic moment tensors of earthquakes occurred after 2015 (in black, see Table 4) and the expected style-of-faulting identified in the same seismic zone (for colors see Figure 6): A - Northern Apennines; B - Eastern Sicily; C - Central and Southern Apennines. Focal mechanisms with a grey background belong to deeper sources. Black numbers indicate the seismic zones, while black numbers refer to seismic events listed in Table 4.

E